

## Geometrically nonlinear dynamic analysis of laminated composite plate using a nonpolynomial shear deformation theory

Babu Ranjan Thakur<sup>1,\*</sup>, Surendra Verma<sup>1</sup>, B.N. Singh<sup>2</sup>, D.K. Maiti<sup>2</sup>

*Department of Aerospace Engineering, Indian Institute of Technology Kharagpur, W. Bengal 721302, India*



### ARTICLE INFO

**Keywords:**

Nonpolynomial shear deformation theory (NPSDT)

Nonlinear dynamic analysis

Green-Lagrange nonlinearity

Steady state analysis

Finite element analysis (FEA)

Laminated composite plate

### ABSTRACT

A computationally efficient  $C^0$  finite element model in conjunction with the nonpolynomial shear deformation theory (NPSDT) is extended to examine the free and forced vibration behavior of laminated composite plates. The employed NPSDT assumes the nonlinear distribution of in-plane displacements which qualify the requirement of traction free boundary conditions at the top and bottom surfaces. The present formulation utilizes both von Kármán and Green-Lagrange type of strain-displacement relations to model the geometric nonlinearity. Using Hamilton's principle, the nonlinear governing equation of motion is derived and then discretized based on the nine-noded Lagrange element. The obtained equations are solved by utilizing unconditionally stable Newmark's scheme in conjunction with Newton-Raphson method. A damping effect in the transient analysis has been introduced in the framework of the Rayleigh damping model. The steady state forced vibration analysis has also been carried out by employing harmonic force with excitation frequency around the natural frequency. The arc-length continuation method is applied to obtain the frequency response. The present model has been validated for a wide range of problems and a detailed numerical study has been carried out for several types of boundary conditions under various types of loading with different magnitude of the load.

### 1. Introduction

Laminated composite materials are becoming one of the most effective and utilized materials for the aerospace, civil, and marine industry, etc. The preference of anisotropic composite material over the conventional isotropic material in a structure can be attributed to the various characteristic of composite materials like high specific modulus, high specific strength, and the tailoring capability for a specific application, etc. In general, composites are extensively utilized like a plate or shell form, which can be designed via three or two dimensional structural analysis. However, two-dimensional structural model which utilizes various plate theories is more preferred due to the high computation requirement of three-dimensional model. The increasing use of laminated composite structure in the industries has necessitated the need for an extensive study to understand the behavior of these structures, which leads to the development of many theories. Moreover, due to the low transverse shear moduli of the laminated composite plate, it possesses a greater transverse shear effect than a homogeneous isotropic plate. Hence, it is essential to incorporate the effect of transverse shear deformation during design, analysis, and

optimization of the laminated composite structures. Addressing this regard, many shear deformation theories have been developed.

The first effort to model the laminated composite is made through the classical laminated plate theory (CLPT), which is an extension of the classical plate theory of Kirchhoff [1]. The problem with the CLPT is that it ignores the transverse shear effect, which is only suitable for thin plates. However, for moderately thick and thick plates, the effect of transverse shear is prominent. Consequently, the prediction made through this method is not free from flaws. For example, CLPT under predicts the deflection and over predicts the frequency and buckling loads for moderately thick plates. Hence, the first-order shear deformation theory (FSDT) is proposed to overcome this problem. The FSDT is based on the Reissner [2] and the Mindlin [3] plate theory, which accommodates the transverse shear effects by taking independent field variable for rotation of transverse normal. Later, a shear correction factor is introduced to equivalently satisfy the traction-free boundary condition at the top and bottom surfaces of plates. However, the value of shear correction factor mainly depends on the material coefficients, geometry, stacking scheme, boundary conditions, and loading conditions, which is difficult to ascertain for practical problems [4]. Later

\* Corresponding author.

E-mail addresses: [brtjsk@iitkgp.ac.in](mailto:brtjsk@iitkgp.ac.in) (B.R. Thakur), [surendraverma2501@iitkgp.ac.in](mailto:surendraverma2501@iitkgp.ac.in) (S. Verma), [bnsingh@aero.iitkgp.ac.in](mailto:bnsingh@aero.iitkgp.ac.in) (B.N. Singh), [dkmaiti@aero.iitkgp.ac.in](mailto:dkmaiti@aero.iitkgp.ac.in) (D.K. Maiti).

<sup>1</sup> Research Scholar.

<sup>2</sup> Professor.

on, in order to overcome the limitations of CLPT and FSDT, several researchers such as Bhimaraddi and Stevens [5], Reddy [6], Ren [7], Kant and Pandya [8], and Mohan et al. [9] developed polynomial higher-order shear deformation theories (HSDTs) which accounts the higher-order terms in the Taylor's expansions of the displacements in the thickness coordinates.

Although several polynomial shear deformation theories have been proposed by many researchers, as mentioned in the above paragraph, the quest for the best approach to predict the structural response efficiently lead the researchers to develop another set of theories, known as nonpolynomial shear deformation theory (NPSDT). Consequently, a nonpolynomial shear deformation theory based on the trigonometric shear strain function was proposed by Touratier [10] to analyze the response of laminated composite plate. His proposed theory carry the same order of complexity as FSDT; however, it is more efficient than the FSDT. Later on, several NPSDTs have been proposed by many researchers such as Aydogdu [11], Karama et al. [12], Meiche et al. [13], and Mantri et al. [14,15], etc. Further, a new nonpolynomial shear deformation theory was proposed by Grover et al. [16] and employed to get the analysis over laminated composite and sandwich plates. Grover et al. [17] investigated the static and buckling response of plate structures based on a new inverse hyperbolic higher-order deformation theory. The theory developed by them is based on the non-linear variation of shear strain through the thickness, which also satisfies the traction free boundary condition at top and bottom surfaces. Further, Sayyad et al. [18] developed a united higher-order sinusoidal theory consists of only four unknowns for the analysis of bending, buckling, and vibration of laminated composite plates. They split the transverse displacement into two components, one for bending and another for shear, to reduce the number of field variables. Moreover, for further in-depth study of various polynomial high order shear deformation theories of multilayered composite plate, a review paper by Abrate and Di Sciuva [19] can be followed. Thus, it is observed from the literature that the nonpolynomial HSDTs are in great use and able to capture the response of structures quite accurately and efficiently.

Apart from the consideration of transverse shear for the laminated composite, considering the geometric nonlinearity is an important aspect for predicting the correct solution of the structural analysis. Further, the thin laminated plate is widely used in the aerospace industry, and it may undergo large deformation and large amplitude vibration on the exertion of severe dynamic loading. Therefore, it is essential to consider the geometric nonlinearity to assess the proper response of such kind of structures. Several researchers studied the geometrically nonlinear structural analysis by incorporating polynomial shear deformation theory, such as Kolli and Chandrashekara [20] studied the nonlinear static and dynamic analysis of stiffened laminated composite plate. They used the von Kármán kinematic relation to model the large deformation. Later, Tanrıöver and Senocak [21] studied the analytical-numerical approach for the large deflection of an unsymmetrically laminated composite plate. Singha and Ganapathi [22] investigated the large amplitude free flexural vibration of laminated composite skew plates. Further, Amabili [23,24] utilized von Kármán nonlinear strain-displacement relations to investigate the large-amplitude vibrations of rectangular plates with different boundary conditions. Kim et al. [25] studied the geometrically nonlinear analysis of laminated composite structures using a 4-node co-rotational shell element with enhanced strains. Kazancı [26] investigated the dynamic response of a sandwich plate under different kinds of time-dependent loads. Further, the geometrically nonlinear dynamic response of laminated composite plate subjected to air blast loading is studied by Susler et al. [27]. Kurtaran [28,29] conducted a geometrically nonlinear transient analysis of laminated composite structures with the generalized differential quadrature method. Moreover, there have been several pieces of literature on the vibration analysis of plates and shells with various shapes and boundary conditions [30,31]. Zhang et al. [32] utilized the element free IMLS-Ritz method to study the geometrically nonlinear large deformation analysis of triangular CNT-reinforced composite

plates. Akgun and Kurtaran [33] utilized the generalized differential quadrature method to study the geometrically nonlinear behavior of laminated composite super-elliptic shell structures. Jafari et al. [34] proposed a novel approximation method for the large deformation analysis of moderately thick fiber-reinforced composite plates. Later, Kant and Swaminathan [35] analyzed the natural frequency of composite and sandwich plates analytically using a higher-order refined theory. Further, Aljani and Amabili [36] studied the geometrically nonlinear bending and forced vibration of plates. They utilized the nonlinearities in membrane and transverse deflection along with the nonlinearities of rotations and thickness. In the same year, Aljani and Amabili [37] studied the nonlinear forced vibration of moderately thick functionally graded (FG) rectangular plate using higher-order shear deformation theory. More recently, Amabili and Reddy [38] proposed a higher-order polynomial theory in which they have included the stretching effect by retaining the nonlinear terms in all the kinematic parameters. From the above literature, it is observed that polynomial shear deformation theory has been widely utilized for transient and steady-state analysis.

Although several research works have been carried out for the dynamic analysis of the laminated composite plate as mentioned above, however, limited work is observed for the damping effect on the transient response. Most of the works are pertaining to viscous damping; for example, Zabarás and Pervez [39] considered the viscous damping approximation to model the damping phenomena in the laminated composite plate structures. Further, Banks and Inman [40] considered four different damping models for composite beams, namely viscous air damping, Kelvin-Voigt damping, time hysteresis damping, and spatial hysteresis damping. They observed that the spatial hysteresis model, combined with viscous air damping, gave the best quantitative agreement with experimental time histories. Further, Pervez and Zabarás [41] studied the transient dynamic and damping analysis of laminated anisotropic plates using a refined plate theory. Further, Latheswary et al. [42] have shown the damping effect on the linear transient response of laminated composite plate utilizing higher-order shear deformation theory. Later, Lei et al. [43] proposed a non-local damping model, including time and spatial hysteresis effects, which is used for the dynamic analysis of structures consisting of Euler-Bernoulli beams and Kirchhoff plates. Further, Ribeiro and Petyt [44,45] have extensively studied the nonlinear forced vibration with the damping model utilizing the harmonic balance method. Azrar et al. [46] studied the nonlinear forced vibration of plates by utilizing the asymptotic method. Kazancı and Mecitoglu [47] studied the nonlinear dynamic analysis of laminated composite plate subjected to blast loading under the structural damping effect. Also, Boumediene et al. [48] investigated the damped nonlinear forced vibrations of thin elastic rectangular plates subjected to harmonic excitation by an asymptotic numerical method. Treviso et al. [49] have presented an extensive review on the damping in composite materials. Further, Amabili et al. [50,51] studied the identification and comparison of damping for large-amplitude vibration of a plate. Aljani et al. [52] proposed the modeling and experimental approach for the damping analysis of large-amplitude vibration of plates. It is observed that a lot of works pertaining to damping have been analyzed for forced vibration steady-state solution.

However, after the extensive literature survey, as per the author's knowledge, it is observed that no work is found for the nonlinear dynamic analysis incorporating von Kármán and Green-Lagrange strain in conjunction with the nonpolynomial shear deformation theory. Therefore, in this paper, finite element solutions for the nonlinear free and forced vibration analysis employing inverse hyperbolic nonpolynomial shear deformation theory are presented. The geometric nonlinearity is included by means of Green-Lagrange and von Kármán strain-displacement relations. The nonlinear Newmark's integration scheme has been used to solve the nonlinear partial differential governing equation. The transient response for various dynamic loading, namely step, sinusoidal, triangular, and exponential load under uniformly and sinusoidally distributed spatial load, have been analyzed. Moreover,

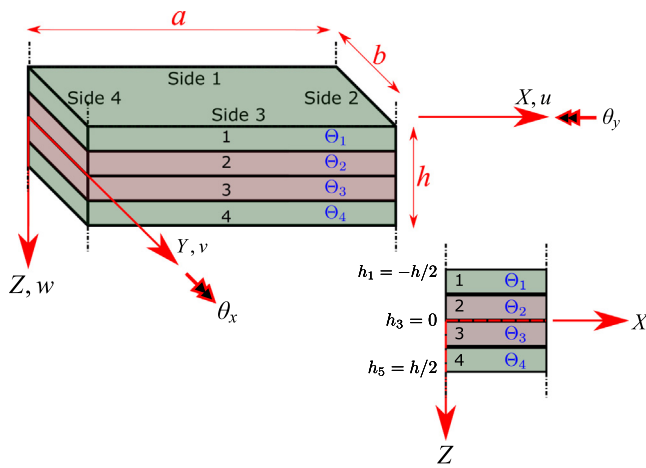


Fig. 1. Schematic diagram of laminated composite plate.

the Rayleigh damping model is utilized to study the damped transient solution for the NPSDT. The phase portraits have also been shown for the better visualization of the damping solution. In addition, the steady-state forced vibration analysis has also been carried out for the excitation frequency around the natural frequency. Concisely, a comprehensive study of geometrically nonlinear dynamic analysis of laminated composite plate has been carried out for the nonpolynomial shear deformation theory.

## 2. Mathematical formulation

A rectangular laminated composite plate of dimension  $a \times b \times h$ , consists of  $n$  orthotropic ply, is arranged in stacking sequence, ( $\Theta_1/\Theta_2/\Theta_3/\Theta_4/\dots$ ). A schematic diagram of laminated composite plate in Cartesian coordinate system ( $X - Y - Z$ ) is shown in Fig. 1.

### 2.1. Displacement field model

To approximate the displacement field, an equivalent single-layer theory is used in the framework of the nonpolynomial shear deformation theory (NPSDT). An inverse hyperbolic shear deformation theory (IHSDT), which has been developed by Grover et al. [16] is employed in particular for demonstration, as the theory in subject is performing quite well over other theory for the static and dynamic analysis [53]. The displacement field model for the same is expressed as follows:

$$\begin{aligned} u(x, y, z) &= u_0(x, y) - z \frac{\partial w_0}{\partial x} + f(z) \theta_x(x, y) \\ v(x, y, z) &= v_0(x, y) - z \frac{\partial w_0}{\partial y} + f(z) \theta_y(x, y) \\ w(x, y, z) &= w_0(x, y) \end{aligned} \quad (1)$$

where  $f(z) = (g(z) + z\Omega)$ ,  $g(z) = \sinh^{-1}\left(\frac{rz}{h}\right)$

$$\text{and } \Omega = \frac{-2r}{h\sqrt{r^2 + 4}}$$

where,  $u_0$ ,  $v_0$ ,  $w_0$  are the mid-plane displacements;  $\theta_x$  and  $\theta_y$  are the shear deformations at the mid-plane. The parameter  $r$  is the transverse shear strain parameter, and  $h$  is the plate thickness. The function  $f(z)$ , is the shear strain function and the plot of the same along the thickness of the plate can be found in Ref. [16].

In Eq. (1), the displacement fields include the derivatives of the field variables which will become second order derivative in the strain. Now,  $C^1$  continuity is required to apply the finite element method. However, achieving  $C^1$  continuity in FEM is a cumbersome process. Hence, requirement of  $C^1$  continuity is reduced to  $C^0$  continuity by imposing an artificial constraint as  $-\partial w_0/\partial x = \phi_x$  and  $-\partial w_0/\partial y = \phi_y$ .

So, after incorporating the artificial constraint, the new displacement field would be

$$\begin{aligned} u(x, y, z) &= u_0(x, y) + z\phi_x + f(z)\theta_x(x, y) \\ v(x, y, z) &= v_0(x, y) + z\phi_y + f(z)\theta_y(x, y) \\ w(x, y, z) &= w_0(x, y) \end{aligned} \quad (2)$$

### 2.2. Strain-displacement relations

The Green-Lagrange state-of-strain,  $\{\epsilon\}$  at a point corresponding to new displacement field, i.e. Eq. (2), in the Cartesian coordinate, is expressed as

$$\{\epsilon\} = \begin{Bmatrix} \epsilon_{xx} \\ \epsilon_{yy} \\ \gamma_{xy} \\ \gamma_{yz} \\ \gamma_{xz} \end{Bmatrix} = \begin{Bmatrix} \frac{\partial u}{\partial x} \\ \frac{\partial v}{\partial y} \\ \frac{\partial u}{\partial y} + \frac{\partial v}{\partial x} \\ \frac{\partial v}{\partial z} + \frac{\partial w}{\partial y} \\ \frac{\partial w}{\partial z} + \frac{\partial u}{\partial x} \end{Bmatrix} + \frac{1}{2} \left\{ 2 \left\{ \frac{\partial u}{\partial x} \frac{\partial u}{\partial y} + \frac{\partial v}{\partial x} \frac{\partial v}{\partial y} + \frac{\partial w}{\partial x} \frac{\partial w}{\partial y} \right\} \right. \\ \left. 2 \left\{ \frac{\partial u}{\partial z} \frac{\partial u}{\partial y} + \frac{\partial v}{\partial z} \frac{\partial v}{\partial y} + \frac{\partial w}{\partial z} \frac{\partial w}{\partial y} \right\} \right. \\ \left. 2 \left\{ \frac{\partial u}{\partial x} \frac{\partial u}{\partial z} + \frac{\partial v}{\partial x} \frac{\partial v}{\partial z} + \frac{\partial w}{\partial x} \frac{\partial w}{\partial z} \right\} \right\} \quad (3)$$

The Green-Lagrange strain, Eq. (3) can be converted into von Kármán strain by retaining the  $(\frac{\partial w}{\partial x})^2$ ,  $(\frac{\partial w}{\partial y})^2$ , and  $(\frac{\partial w}{\partial z})^2$  terms of the nonlinear part to be nonzero while all other terms of the nonlinear part set to be zero. Further, due to the consideration of orthotropic material in present study, the strain vector,  $\{\epsilon\}$  can be decoupled into in-plane strain vector,  $\{\epsilon_b\}$  and transverse vector,  $\{\epsilon_s\}$  as

$$\{\epsilon\} = \begin{Bmatrix} \epsilon_b \\ \epsilon_s \end{Bmatrix} = \begin{Bmatrix} \epsilon_{bl} \\ \epsilon_{sl} \end{Bmatrix} + \begin{Bmatrix} \epsilon_{bnl} \\ \epsilon_{snl} \end{Bmatrix} \quad (4)$$

where,

$$\begin{Bmatrix} \epsilon_{bl} \\ \epsilon_{sl} \end{Bmatrix} = \begin{Bmatrix} Z_{bl} \hat{\epsilon}_{bl} \\ Z_{sl} \hat{\epsilon}_{sl} \end{Bmatrix} \quad (5)$$

in which,

$$\hat{\epsilon}_{bl} = \begin{Bmatrix} \frac{\partial u_0}{\partial x} \\ \frac{\partial v_0}{\partial y} \\ \frac{\partial u_0}{\partial y} + \frac{\partial v_0}{\partial x} \\ \frac{\partial \phi_x}{\partial x} \\ \frac{\partial \phi_y}{\partial y} \\ \frac{\partial \phi_x}{\partial y} + \frac{\partial \phi_y}{\partial x} \\ \frac{\partial \theta_x}{\partial x} \\ \frac{\partial \theta_y}{\partial y} \\ \frac{\partial \theta_x}{\partial y} + \frac{\partial \theta_y}{\partial x} \end{Bmatrix} \quad \text{and} \quad \hat{\epsilon}_{sl} = \begin{Bmatrix} \frac{\partial w_0}{\partial y} + \phi_y \\ \frac{\partial w_0}{\partial x} + \phi_x \\ \theta_y \\ \theta_x \end{Bmatrix} \quad (6)$$

and

$$\begin{aligned} Z_{bl} &= \begin{bmatrix} 1 & 0 & 0 & z & 0 & 0 & f(z) & 0 & 0 \\ 0 & 1 & 0 & 0 & z & 0 & 0 & f(z) & 0 \\ 0 & 0 & 1 & 0 & 0 & z & 0 & 0 & f(z) \end{bmatrix}, \\ Z_{sl} &= \begin{bmatrix} 1 & 0 & f'(z) & 0 \\ 0 & 1 & 0 & f'(z) \end{bmatrix} \end{aligned}$$

Similarly, for the nonlinear strain relations

$$\begin{Bmatrix} \epsilon_{bnl} \\ \epsilon_{snl} \end{Bmatrix} = \frac{1}{2} \begin{Bmatrix} Z_{bnl} \hat{\epsilon}_{bnl} \\ Z_{snl} \hat{\epsilon}_{snl} \end{Bmatrix} = \frac{1}{2} \begin{Bmatrix} Z_{bnl} A_b \phi_b \\ Z_{snl} A_s \phi_s \end{Bmatrix} \quad (7)$$

and

$$\begin{Bmatrix} \delta \epsilon_{bnl} \\ \delta \epsilon_{snl} \end{Bmatrix} = \begin{Bmatrix} Z_{bnl} \delta \hat{\epsilon}_{bnl} \\ Z_{snl} \delta \hat{\epsilon}_{snl} \end{Bmatrix} = \begin{Bmatrix} Z_{bnl} A_b \delta \phi_b \\ Z_{snl} A_s \delta \phi_s \end{Bmatrix} \quad (8)$$

where  $Z_{bnl}$ ,  $Z_{snl}$  are given in Box I.

The expressions for  $A_b \phi_b$  and  $A_s \phi_s$  are given in the Appendix A.

$$\mathbf{Z}_{bnl} = \begin{bmatrix} 1 & 0 & 0 & z & 0 & 0 & f(z) & 0 & 0 & zf(z) & 0 & 0 & z^2 & 0 & 0 & f^2(z) & 0 \\ 0 & 1 & 0 & 0 & z & 0 & 0 & f(z) & 0 & 0 & zf(z) & 0 & 0 & z^2 & 0 & 0 & f^2(z) & 0 \\ 0 & 0 & 1 & 0 & 0 & z & 0 & 0 & f(z) & 0 & 0 & zf(z) & 0 & 0 & z^2 & 0 & 0 & f^2(z) \\ 1 & 0 & z & 0 & f(z) & 0 & f'(z) & 0 & zf'(z) & 0 & f(z)f'(z) & 0 & 0 & f(z)f'(z) & 0 & 0 & f(z)f'(z) \end{bmatrix}$$

$$\mathbf{Z}_{snl} = \begin{bmatrix} 1 & 0 & z & 0 & f(z) & 0 & f'(z) & 0 & zf'(z) & 0 & f(z)f'(z) & 0 & 0 & f(z)f'(z) & 0 & 0 & f(z)f'(z) \\ 0 & 1 & 0 & z & 0 & f(z) & 0 & f'(z) & 0 & zf'(z) & 0 & f(z)f'(z) & 0 & 0 & f(z)f'(z) & 0 & 0 & f(z)f'(z) \end{bmatrix}$$

Box I.

### 2.3. Constitutive equation

The Hooke's law to represent the constitutive equation of  $k$ th arbitrary orthotropic layer in X-Y-Z coordinate system for plate problem (hypothetically  $\sigma_z = 0$ ) is given by

$$\{\sigma\}^{(k)} = [\mathcal{T}_{trans}^{(k)}] [\mathbf{Q}] [\mathcal{T}_{trans}^{(k)}]^T \{\epsilon\} = [\bar{\mathbf{Q}}]^{(k)} \{\epsilon\}^{(k)} \quad (9)$$

which can be further expanded as

$$\begin{cases} \sigma_{xx} \\ \sigma_{yy} \\ \sigma_{xy} \\ \sigma_{yz} \\ \sigma_{xz} \end{cases}^{(k)} = [\mathcal{T}_{trans}^{(k)}] \begin{bmatrix} Q_{11} & Q_{12} & Q_{16} & 0 & 0 \\ Q_{21} & Q_{22} & Q_{26} & 0 & 0 \\ Q_{61} & Q_{62} & Q_{66} & 0 & 0 \\ 0 & 0 & 0 & Q_{44} & Q_{45} \\ 0 & 0 & 0 & Q_{54} & Q_{55} \end{bmatrix} [\mathcal{T}_{trans}^{(k)}]^T \begin{cases} \epsilon_{xx} \\ \epsilon_{yy} \\ \gamma_{xy} \\ \gamma_{yz} \\ \gamma_{xz} \end{cases}^{(k)} \quad (10)$$

where,  $\{\sigma\}$ ,  $\{\epsilon\}$  and  $[\mathbf{Q}]$  are stress vector, strain vector and material constants in the global coordinate, respectively. And the transformation matrix to convert 1-2-3 coordinate system to X-Y-Z coordinate system is denoted by  $[\mathcal{T}_{trans}]$  [54]. Further, the symmetry in the orthotropic material leads to  $Q_{21} = Q_{12}$ ,  $Q_{61} = Q_{16}$ ,  $Q_{62} = Q_{26}$ , and  $Q_{54} = Q_{45}$ .

Each material matrix coefficient can be expressed as

$$Q_{11} = \frac{E_1}{1 - v_{12}v_{21}}, \quad Q_{12} = \frac{v_{12}E_2}{1 - v_{12}v_{21}}, \quad Q_{22} = \frac{E_2}{1 - v_{12}v_{21}}$$

$$Q_{66} = G_{12}, \quad Q_{44} = G_{23}, \quad Q_{55} = G_{13}$$

where,  $E_1$  and  $E_2$  are the Young's modulus in the longitudinal and transverse fiber direction, respectively;  $G_{12}$ ,  $G_{23}$ ,  $G_{13}$  are the shear modulus;  $v_{12}$  and  $v_{21}$  are major and minor Poisson's ratios; subscripts 1 denote the longitudinal fiber direction, whereas 2,3 represents the transverse direction of fiber. Further, the resulting in-plane and transverse stresses are defined and shown in the Appendix B.

### 2.4. Equation of motion

For arbitrary space variable and admissible virtual displacement  $\delta\{u, v, w\}$ , Hamilton's principle of the given system using total Lagrangian approach is written as

$$\delta \int_{t_i}^{t_f} \mathcal{L} dt = \int_{t_i}^{t_f} (\delta \mathcal{K} - \delta \mathcal{U} + \delta \mathcal{W}_{ext}) dt = 0 \quad (11)$$

**Strain energy.** The virtual strain energy of plate due to mechanical strain and the artificial constraints is expressed as,

$$\delta \mathcal{U} = \int_V \delta \{\epsilon\}^T \{\sigma\} dV + \delta \mathcal{U}_\gamma \quad (12)$$

where  $\delta \mathcal{U}_\gamma$  is the virtual strain energy due to artificial constraints with penalty parameter,  $\gamma$  and is expressed as

$$\delta \mathcal{U}_\gamma = \gamma \int_V \left\{ \delta \left( \phi_x + \frac{\partial w_0}{\partial x} \right)^T \left( \phi_x + \frac{\partial w_0}{\partial x} \right) + \delta \left( \phi_y + \frac{\partial w_0}{\partial y} \right)^T \left( \phi_y + \frac{\partial w_0}{\partial y} \right) \right\} dV \quad (13)$$

**Kinetic energy.** The virtual kinetic energy of the system is expressed as follows

$$\int_{t_i}^{t_f} \delta \mathcal{K} dt = - \int_{t_i}^{t_f} \int_V \rho \delta \{\mathbf{u}\}^T \{\ddot{\mathbf{u}}\} dV dt \quad (14)$$

where,  $\rho$  is the mass density of the material, and  $t_i$ ,  $t_f$  are the initial and final time of consideration for analysis, respectively.

**Work done by external forces.** The virtual work done by transverse mechanical loading,  $P$  is written as

$$\delta \mathcal{W}_{ext} = \int_A \delta \mathbf{w}^T P dA \quad (15)$$

### 2.5. Finite element formulation

For finite element discretization, a nine-noded isoparametric element with seven degrees of freedom (DOFs) per node is considered. The present finite element utilizes same Lagrange basis function for both generalization of field variables and geometry; and described as

$$\{\mathbf{u}\} = \sum_{i=1}^9 N_i \mathbf{q}_i, \quad x = \sum_{i=1}^9 N_i x_i, \quad y = \sum_{i=1}^9 N_i y_i \quad (16)$$

where,  $\{\mathbf{u}\} = \{u_0, v_0, w_0, \phi_x, \theta_x, \phi_y, \theta_y\}^T$  is the generalized field variable,  $\mathbf{q}_i$  is the corresponding nodal field variables associated with  $i$ th node,  $(x, y)$  are the generalized geometric coordinates, and  $x_i$  and  $y_i$  are the geometric coordinate values of the corresponding  $i$ th node.

Using the expression of displacement vector,  $\{\mathbf{u}\}$  from Eq. (16), the generalized linear bending strain vector,  $\hat{\epsilon}_{bl}$  and the generalized linear shear strain vector,  $\hat{\epsilon}_{sl}$  at any point can be written as

$$\hat{\epsilon}_{bl} = \mathbf{B}_{bl} \mathbf{q} = \sum_{i=1}^9 \mathbf{B}_{bli} \mathbf{q}_i \quad \hat{\epsilon}_{sl} = \mathbf{B}_{sl} \mathbf{q} = \sum_{i=1}^9 \mathbf{B}_{sli} \mathbf{q}_i \quad (17)$$

where

$$\{\mathbf{q}\} = \{\mathbf{q}_1^T \quad \mathbf{q}_2^T \quad \dots \quad \mathbf{q}_8^T \quad \mathbf{q}_9^T\}^T$$

$$\mathbf{q}_i = \{u_{0i} \quad v_{0i} \quad w_{0i} \quad \phi_{xi} \quad \phi_{yi} \quad \theta_{xi} \quad \theta_{yi}\}^T$$

Similarly, for the nonlinear terms

$$\hat{\epsilon}_{bnl} = \mathbf{B}_{bnl} \mathbf{q} = \sum_{i=1}^9 \mathbf{B}_{bni} \mathbf{q}_i = \sum_{i=1}^9 \mathbf{A}_b \mathbf{G}_{bni} \mathbf{q}_i \quad (18)$$

$$\hat{\epsilon}_{snl} = \mathbf{B}_{snl} \mathbf{q} = \sum_{i=1}^9 \mathbf{B}_{sni} \mathbf{q}_i = \sum_{i=1}^9 \mathbf{A}_s \mathbf{G}_{sni} \mathbf{q}_i$$

and the expression of  $\mathbf{B}_{bli}$ ,  $\mathbf{B}_{sli}$ ,  $\mathbf{G}_{bni}$ , and  $\mathbf{G}_{sni}$  is presented in the Appendix C

**Stiffness matrix.** The elemental stiffness matrix of the laminated plate is given by

$$\mathbf{K} = \int_\Omega (\mathbf{B}_{bl}^T \mathbf{D}_{lbl} \mathbf{B}_{bl} + \frac{1}{2} \mathbf{B}_{bl}^T \mathbf{D}_{lbnl} \mathbf{B}_{bnl} + \mathbf{B}_{bnl}^T \mathbf{D}_{nlbl} \mathbf{B}_{bl} + \frac{1}{2} \mathbf{B}_{bnl}^T \mathbf{D}_{nlnl} \mathbf{B}_{bnl} \mathbf{B}_{bnl}^T \mathbf{D}_{nlbnl} \mathbf{B}_{bnl} + \mathbf{B}_{sl}^T \mathbf{D}_{lsl} \mathbf{B}_{sl} + \frac{1}{2} \mathbf{B}_{sl}^T \mathbf{D}_{lsnl} \mathbf{B}_{snl} + \mathbf{B}_{snl}^T \mathbf{D}_{nsl} \mathbf{B}_{sl} + \frac{1}{2} \mathbf{B}_{snl}^T \mathbf{D}_{nsnl} \mathbf{B}_{snl}) d\Omega + \mathbf{K}_\gamma \quad (19)$$

in which

$$\begin{aligned} D_{lbl} &= \int_{-\frac{h}{2}}^{\frac{h}{2}} Z_{bl}^T \bar{Q}_b Z_{bl} dz, \quad D_{lbnl} = \int_{-\frac{h}{2}}^{\frac{h}{2}} Z_{bl}^T Q_b Z_{bnl} dz, \\ D_{nlbl} &= \int_{-\frac{h}{2}}^{\frac{h}{2}} Z_{bnl}^T \bar{Q}_b Z_{bl} dz, \quad D_{nlbnl} = \int_{-\frac{h}{2}}^{\frac{h}{2}} Z_{bnl}^T Q_b Z_{bnl} dz, \\ D_{lsl} &= \int_{-\frac{h}{2}}^{\frac{h}{2}} Z_{sl}^T \bar{Q}_s Z_{sl} dz, \quad D_{tsnl} = \int_{-\frac{h}{2}}^{\frac{h}{2}} Z_{sl}^T \bar{Q}_s Z_{snl} dz, \\ D_{nisl} &= \int_{-\frac{h}{2}}^{\frac{h}{2}} Z_{snl}^T \bar{Q}_s Z_{sl} dz, \quad D_{ntslnl} = \int_{-\frac{h}{2}}^{\frac{h}{2}} Z_{snl}^T \bar{Q}_s Z_{snl} dz \end{aligned}$$

and the expression for penalty stiffness matrix,  $\mathbf{K}_\gamma$  is

$$\mathbf{K}_\gamma = \int_A \gamma \mathbf{B}_\gamma^T \mathbf{B}_\gamma h dA$$

where

$$\mathbf{B}_\gamma q = \mathbf{B}_{\gamma i} q_i$$

in which

$$\mathbf{B}_{\gamma i} = \begin{bmatrix} 0 & 0 & \frac{\partial N_i}{\partial y} & N_i & 0 & 0 & 0 \\ 0 & 0 & \frac{\partial N_i}{\partial x} & 0 & N_i & 0 & 0 \end{bmatrix}$$

To avoid ill-conditioning of the stiffness matrix,  $\mathbf{K}$  derived from mechanical strain energy and strain energy due to penalty, and to ensure the accuracy of the analysis, the selection of penalty parameter plays an important role. Generally penalty is taken as large as possible compatible with the computer hardware architecture for software implementation. However, in this analysis penalty parameter is taken in the order of transverse elastic modulus,  $E_2$ .

**Mass matrix.** The expression of elemental mass matrix is given as

$$\mathbf{M} = \int_A \mathbf{R}^T \mathbf{m} \mathbf{R} dA \quad (20)$$

where

$$\mathbf{m} = \int_{-h/2}^{h/2} \rho \begin{bmatrix} 1 & 0 & 0 & z & 0 & f(z) & 0 \\ 0 & 1 & 0 & 0 & z & 0 & f(z) \\ 0 & 0 & 1 & 0 & 0 & 0 & 0 \\ z & 0 & 0 & z^2 & 0 & zf(z) & 0 \\ 0 & z & 0 & 0 & z^2 & 0 & zf(z) \\ f(z) & 0 & 0 & zf(z) & 0 & f(z)^2 & 0 \\ 0 & f(z) & 0 & 0 & zf(z) & 0 & f(z)^2 \end{bmatrix} dz$$

and

$$\mathbf{R}q = \sum_{i=1}^9 N_i \mathbf{I}_7 q_i$$

in which,  $\mathbf{I}_7$  is the identity matrix of order seven.

**Elemental load vector.** The elemental load vector for distributed traction load,  $P$  is given as

$$\mathbf{F}_m = \int \mathbf{W}^T P dA \quad (21)$$

where

$$\mathbf{W} = \{ \mathbf{W}_1 \quad \mathbf{W}_2 \quad \mathbf{W}_3 \quad \mathbf{W}_4 \quad \mathbf{W}_5 \quad \mathbf{W}_6 \quad \mathbf{W}_7 \quad \mathbf{W}_8 \quad \mathbf{W}_9 \}$$

in which

$$\mathbf{W}_i = [0 \quad 0 \quad N_i \quad 0 \quad 0 \quad 0 \quad 0]$$

**Governing equation.** To obtain the governing equations, Eqs. (12), (14) and (15) are substituted in Eq. (11), and then finite element discretization is employed using Eq. (16). After eliminating the virtual displacement,  $\delta q$ , the system of equations of motion can be obtained in the following matrix form

$$\mathbf{M} \ddot{\mathbf{q}} + \mathbf{K} \mathbf{q} = \mathbf{F}_m \quad (22)$$

The governing set of equations for eigenvalue characterization of the system is obtained as

$$\mathbf{M} \ddot{\mathbf{q}} + \mathbf{K} \mathbf{q} = \mathbf{0} \quad (23)$$

In general, mechanical system possess inherent damping property, however, it is very difficult to exactly model the damping characteristic. In practice, damping ratio is obtained experimentally for various modes. Then using these damping ratio for particular frequency range damping is modeled using Rayleigh damping, which is a special case of the Caughey series [55].

Rayleigh damping is also known as proportional damping or classical damping model which expresses damping as a linear combination of the mass and stiffness matrices, that is,

$$\mathbf{C} = \alpha \mathbf{M} + \beta \mathbf{K}_L \quad (24)$$

where  $\alpha$  and  $\beta$  are Rayleigh damping coefficients, and  $\mathbf{K}_L$  is the linear stiffness matrix.

The value of Rayleigh damping coefficient for a particular frequency bandwidth can be calculated from following given equation as

$$\xi_n = \frac{\alpha}{2} \frac{1}{\omega_n} + \frac{\beta}{2} \omega_n \quad (25)$$

where,  $\xi_n$  is the damping ratio and  $\omega_n$  is the natural frequency of  $n$ th mode. For two selected  $i$ th and  $j$ th mode,  $\alpha$  and  $\beta$  can be obtained as

$$\begin{Bmatrix} \alpha \\ \beta \end{Bmatrix} = \begin{bmatrix} \frac{1}{2\omega_i} & \frac{\omega_i}{2} \\ \frac{1}{2\omega_j} & \frac{\omega_j}{2} \end{bmatrix}^{-1} \begin{Bmatrix} \xi_i \\ \xi_j \end{Bmatrix} \quad (26)$$

Thus, after consideration of viscous damping, the equation of motion becomes

$$\mathbf{M} \ddot{\mathbf{q}} + \mathbf{C} \dot{\mathbf{q}} + \mathbf{K} \mathbf{q} = \mathbf{F}_m \quad (27)$$

## 2.6. Solution process

For nonlinear transient analysis, an initial value problem in time,  $t$  is solved using nonlinear Newmark's algorithm. In this nonlinear Newmark's scheme for each time step, the Newton-Raphson method is used to solve the nonlinear algebraic equations. The solution is obtained by following the detailed steps given by Krenk [56].

There is a requirement of tangent stiffness matrix,  $\mathbf{K}_T$  in the Newmark's algorithm, which is defined as

$$\mathbf{K}_T = \mathbf{K}_L + \mathbf{K}_{NL} + \mathbf{K}_\sigma \quad (28)$$

where  $\mathbf{K}_\sigma$  is the initial stiffness matrix due to initial stresses at particular time.

The combined expression for  $\mathbf{K}_L + \mathbf{K}_{NL}$  is given by

$$\begin{aligned} \mathbf{K}_L + \mathbf{K}_{NL} &= \int_\Omega (\mathbf{B}_{bl}^T D_{lbl} \mathbf{B}_{bl} + \mathbf{B}_{bl}^T D_{lbnl} \mathbf{B}_{bnl} + \mathbf{B}_{bnl}^T D_{nlbl} \mathbf{B}_{bl} \\ &\quad + \mathbf{B}_{bnl}^T D_{nlbnl} \mathbf{B}_{bnl} \\ &\quad + \mathbf{B}_{sl}^T D_{lsl} \mathbf{B}_{sl} + \mathbf{B}_{sl}^T D_{tsnl} \mathbf{B}_{snl} + \mathbf{B}_{snl}^T D_{nisl} \mathbf{B}_{sl} \\ &\quad + \mathbf{B}_{snl}^T D_{ntslnl} \mathbf{B}_{snl}) d\Omega + \mathbf{K}_\gamma \end{aligned} \quad (29)$$

and, the expression for  $\mathbf{K}_\sigma$  is given by

$$\mathbf{K}_\sigma = \int_\Omega (\mathbf{G}_{bnli}^T \mathbf{S}_b \mathbf{G}_{bnli} + \mathbf{G}_{snli}^T \mathbf{S}_s \mathbf{G}_{snli}) d\Omega \quad (30)$$

in which,  $\mathbf{S}_b$  and  $\mathbf{S}_s$  are given in the Appendix D.

To solve the eigenvalue problem, i.e., nonlinear free vibration, a direct iterative method is employed to obtain the nonlinear frequency ratio. In this, for first iteration, the linear eigenvalue problem is solved for eigenvalue and normalized eigenvector considering  $\mathbf{q} = 0$ . For further iteration, eigenvector is scaled according to the specified amplitude ratio at a particular spatial location, usually center of the plate. Then, eigenvalue problem is again solved by considering this scaled normalized eigenvector to calculate the new normalized eigenvector and corresponding eigenvalue until relative error of natural frequency is less than prescribed tolerance, say  $10^{-2}$  or otherwise stated.

### 3. Results and discussions

In the present study the nine-noded quadrilateral isoparametric element is employed. The selective integration, that is, the  $2 \times 2$  Gauss rule is used to integrate the shear energy and nonlinear strain terms, and the  $3 \times 3$  Gauss rule is applied to integrate the bending and inertia terms. There are three parts of the result. In the first part, free vibration analysis result has been presented and in the second part, transient analysis has been shown. Whereas in the third part, steady state forced vibration for the excitation frequency around the neighborhood of fundamental natural frequency has been shown.

#### 3.1. Material properties

Following sets of material properties are used in the analysis:

- MM1 [57]:  $E_1 = E_2 = E_3 = 63$  GPa,  $\nu_{12} = \nu_{21} = \nu_{13} = 0.3$ ,  $G_{12} = G_{23} = G_{13} = 24.2$  GPa,  $\rho = 7600$  kg/m<sup>3</sup>
- MM2 [58]:  $E_1 = 40E_2$ ,  $\nu_{12} = 0.25$ ,  $G_{12} = 0.6 \times E_2$ ,  $G_{13} = G_{12}$ ,  $G_{23} = 0.5 \times E_2$ ,  $\rho = 8 \times 10^{-6}$  N s/cm<sup>4</sup> (800 kg/m<sup>3</sup>)
- MM3 [59,60]:  $E_2 = 21$  GPa,  $E_1 = 525$  GPa,  $G_{12} = G_{13} = G_{23} = 10.5$  GPa,  $\nu_{12} = 0.25$ ,  $\rho = 800$  kg/m<sup>3</sup>
- MM4 [59]:  $E_1 = 172.369$  GPa,  $E_2 = 6.895$  GPa,  $G_{12} = 3.448$  GPa,  $G_{13} = G_{12}$ ,  $G_{23} = 1.379$  GPa,  $\nu_{12} = 0.25$ ,  $\rho = 1603.03$  kg/m<sup>3</sup>
- MM5 [42]:  $E_1 = 25E_2$ ,  $E_2 = 2.1 \times 10^6$  N/cm<sup>2</sup>,  $G_{12} = G_{13} = 0.5E_2$ ,  $G_{23} = 0.2E_2$ ,  $\nu_{12} = 0.25$ ,  $\rho = 8 \times 10^{-6}$  N s<sup>2</sup>/cm<sup>4</sup> (800 kg/m<sup>3</sup>)

#### 3.2. Various type of loading

The analysis of laminated composite plate is considered under the application of various time-dependent blast pulse load. These loads are defined and expressed as follows:

- Step Loading

$$F(t) = \begin{cases} 1, & 0 \leq t \leq t_1 \\ 0, & t > t_1 \end{cases}$$

where  $t_1$  is the positive phase duration of load.

- Sinusoidal Loading

$$F(t) = \begin{cases} \sin(\pi t/t_1), & 0 \leq t \leq t_1 \\ 0, & t > t_1 \end{cases}$$

- Explosive Blast Loading or Exponential Loading

$$F(t) = \begin{cases} e^{-\gamma t}, & 0 \leq t \leq t_1 \\ 0, & t > t_1 \end{cases}$$

where,  $\gamma$  denotes a decay parameter. The value of  $\gamma = 660$  s<sup>-1</sup> has been considered.

- Triangular Loading

$$F(t) = \begin{cases} 1 - t/t_1, & 0 \leq t \leq t_1 \\ 0, & t > t_1 \end{cases}$$

- The spatial pressure applied for the analysis are defined by

$$P(x, y, t)$$

$$= \begin{cases} q_0 \sin(\pi x/a) \sin(\pi y/b) F(t), & \text{Sinusoidal Distributed Loading} \\ q_0 F(t), & \text{Uniformly Distributed Loading} \end{cases}$$

in which,  $q_0$  is the loading intensity.

**Table 1**

Different strain function,  $f(z) = g(z) + z\Omega$ , used in the present work.

Source	$g(z)$	$\Omega$	Parameter value
IHSDT [16]	$\sinh^{-1}(\frac{z}{h})$	$-\frac{2r}{h\sqrt{r^2+4}}$	$r = 3$
Reddy's TSDT [6]	$z - \frac{4}{3h^2} z^3$	0	
TEHSDT [61]	$\tan(\frac{\pi z}{2h}) m^{\sec(\frac{\pi z}{2h})}$	$-\frac{\pi m\sqrt{2}}{m\sqrt{2}} (\sqrt{2} + \ln(m))$	$m = 0.03$
Touratier's theory [62]	$\frac{h}{\pi} \sin(\frac{\pi z}{h})$	0	

#### 3.3. Boundary conditions

In the displacement approach formulation, only kinematic constraints are need to be satisfied for imposition of boundary conditions, i.e.,  $(u_0, v_0, w_0, \phi_x, \phi_y, \theta_x, \theta_y)$ . The different types of boundary conditions, most commonly occurring in practice are considered for finite element analysis of laminated composite plate to assess the efficacy of present approach and the same are elucidated below.

- Simply Supported

1. For cross-ply

$$\text{SSSS-1: } v_0 = w_0 = \phi_y = \theta_y = 0 \text{ at } x = 0, a \text{ and} \\ u_0 = w_0 = \phi_x = \theta_x = 0 \text{ at } y = 0, b$$

2. For angle-ply

$$\text{SSSS-2: } u_0 = w_0 = \phi_x = \theta_y = 0 \text{ at } x = 0, a \text{ and} \\ v_0 = w_0 = \phi_y = \theta_x = 0 \text{ at } y = 0, b$$

3. Immovable hard (Hinged)

$$\text{SSSS-3: } u_0 = v_0 = w_0 = \phi_y = \theta_y = 0 \text{ at } x = 0, a \text{ and} \\ u_0 = v_0 = w_0 = \phi_x = \theta_x = 0 \text{ at } y = 0, b$$

4. Immovable soft

$$\text{SSSS-4: } u_0 = v_0 = w_0 = 0 \text{ at } x = 0, a \text{ and} \\ u_0 = v_0 = w_0 = 0 \text{ at } y = 0, b$$

- Clamped boundary condition

$$\text{CCCC: } u_0 = v_0 = w_0 = \phi_x = \phi_y = \theta_x = \theta_y = 0 \text{ at } x = 0, a \text{ and} \\ y = 0, b.$$

#### 3.4. Free vibration analysis

The geometrically nonlinear free vibration analysis of laminated composite plate utilizing von Kármán and Green–Lagrange strain-displacement relation, which accounts for the coupling between bending and membrane behavior, is extensively carried out. This coupling between bending and membrane behavior contributes to plate stiffening, which results in an increase in the magnitude of nonlinear frequency when compared with linear results. To demonstrate this effect, nonlinear frequency ratio,  $(\bar{\omega}_{nl}/\bar{\omega}_l)$  has been evaluated for both von Kármán and Green–Lagrange sense of nonlinearity. The linear nondimensionalized fundamental frequency is given by  $\bar{\omega}_l = (\omega a^2/h)\sqrt{\rho/E_2}$ . The equilibrium equations are solved by a direct-iterative approach for each amplitude ratio,  $(w_{max}/h)$ . The iteration is repeated until the frequency error between two consecutive iterations reduces to the desired error tolerance  $\|\omega_{i+1} - \omega_i\|/\|\omega_i\| < 10^{-2}$  unless stated otherwise in the problem. Several nonpolynomial shear deformation theories, namely inverse hyperbolic shear deformation theory (IHSDT), third-order shear deformation theory (Reddy's TSDT), tangential–exponential higher-order shear deformation theory (TEHSDT), and trigonometric shear deformation theory (Touratier's theory) are utilized for the nonlinear free vibration analysis, and the strain functions for the same are listed in Table 1.

##### 3.4.1. Nonlinear free vibration of simply supported square isotropic plate

Nonlinear frequency ratios of a moderately thick simply supported (SSSS-3) isotropic plate having material properties MM1 are calculated for both the von Kármán and Green–Lagrange strains. The plate has a side-to-thickness ratio,  $a/h = 10$ . The obtained nonlinear frequency

**Table 2**

Nonlinear frequency ratio ( $\bar{\omega}_{nl}/\bar{\omega}_l$ ) of the simply supported (SSSS-3) isotropic square plate.

Source/Method	$w_{max}/h$				
	0.2	0.4	0.6	0.8	1.0
Ref. [57]	1.0256	1.0975	1.2103	1.3582	1.5321
Ganapathi et al. [63]	1.0266	1.1019	1.2194	1.3704	1.5414
Sarma [64]	1.0259	1.1002	1.2149	1.3632	1.5345
IHSDT <sup>a</sup>	1.02750	1.10638	1.22769	1.38196	1.56177
IHSDT <sup>b</sup>	1.02903	1.11382	1.24294	1.40637	1.59604
Reddy's TSDT <sup>a</sup>	1.02751	1.10644	1.22781	1.38216	1.56208
Reddy's TSDT <sup>b</sup>	1.02905	1.1139	1.2431	1.40662	1.59639
TEHSDT <sup>a</sup>	1.02751	1.10641	1.22776	1.38207	1.56194
TEHSDT <sup>b</sup>	1.02904	1.11386	1.24301	1.40649	1.59621
Touratier's theory <sup>a</sup>	1.02751	1.10644	1.2278	1.38215	1.56206
Touratier's theory <sup>b</sup>	1.02905	1.11389	1.24308	1.40659	1.59635

<sup>a</sup>von Kármán.

<sup>b</sup>Green–Lagrange for different theories.

ratios, ( $\bar{\omega}_{nl}/\bar{\omega}_l$ ) for the first mode at various amplitude-to-thickness ratios ( $w_{max}/h$ ) of the isotropic plate are shown in **Table 2**. The present results have been compared with the available solution in the literature [57,63,64]. It is observed that the present von Kármán and Green–Lagrange solutions for various shear deformation theories, as mentioned in **Table 1**, are in well agreement with the available solution. The obtained nonlinear frequency ratios for different theories are found to be almost the same due to the isotropic plate being less sensitive for the shear effect than the laminated plate. Moreover, the solutions obtained by the consideration of Green–Lagrange strain show more contribution of nonlinearity and hence the nonlinear frequency ratios, ( $\bar{\omega}_{nl}/\bar{\omega}_l$ ) are found to be higher than the von Kármán. These results confirm the validation of the present finite element formulation for both von Kármán and Green–Lagrange strain. It is also observed from the **Table 2** that the increase in amplitude ratio increases the rate of nonlinearity (increase of frequency ratio with respect to amplitude ratio). As the amplitude ratio ( $w_{max}/h$ ) is used to scale the obtained eigenvector which is fed back to calculate nonlinear stiffness matrix, and hence, the increase in amplitude ratio increases the nonlinear stiffness, due to which, increase in nonlinear frequency is observed.

#### 3.4.2. Effect of span to thickness ratio on nonlinear free vibration of laminated composite plate

The effect of span-to-thickness ratio,  $a/h$  for various amplitude ratio ( $w_{max}/h$ ) on the geometrically nonlinear free vibration behavior of eight-layered square cross-ply ( $0^\circ/90^\circ/0^\circ/90^\circ_s$ ) and angle-ply ( $45^\circ/-45^\circ/45^\circ/-45^\circ_s$ ) laminated plates, under simply supported (SSSS – 3) boundary conditions, is demonstrated in **Tables 3** and **4** for various theories mentioned in **Table 1**. The material properties of each lamina are considered as MM2 with  $E_2 = 10^6 \text{ N/cm}^2$ . It is observed from **Tables 3** and **4** that the available results [58,65] overestimate the nonlinear vibration response of the laminated plate. Also, it can be seen that the degree of nonlinearity increases as the amplitude ratio ( $w_{max}/h$ ) increases, but the nonlinearity decreases as the  $a/h$  ratio increases, as mentioned in **Tables 3** and **4**. The reason is, as  $a/h$  ratio increase, i.e., the plate gets thinner, the extensional stiffness matrix (proportional to  $h$ ) decreases, which reduces the effect of nonlinearity, and the same is observed in the results. Also, from the present von Kármán and Green–Lagrange free vibration results, it can be seen that the Green–Lagrange nonlinear frequency ratio ( $\bar{\omega}_{nl}/\bar{\omega}_l$ ) is greater than the von Kármán nonlinear frequency ratio because the additional terms in strain–displacement relation give rise to more stiffening effect. The obtained result is validated with the available results in the literature [58,65]. Further, it can be observed that the obtained solution for different higher-order polynomial and nonpolynomial shear deformation theories are having little difference, and IHSDT solution is found to be the lowest one. The lowest value of the IHSDT solution among other theories suggests the better performance of IHSDT, as

**Table 3**

Nonlinear frequency ratio ( $\bar{\omega}_{nl}/\bar{\omega}_l$ ) for a simply supported (SSSS – 3) cross-ply ( $0^\circ/90^\circ/0^\circ/90^\circ_s$ ) square laminated plate.

a/h	Source/Method	$w_{max}/h$			
		0.1	0.2	0.3	0.4
5	FSDT [58]	1.0346	1.1083	1.2332	–
	HSDT 7DOF [58]	1.0279	1.1083	1.2332	–
	FEM-ITS DT 7DOF [65]	1.0278	1.1081	1.2330	1.2828
	IHSDT <sup>a</sup>	1.02736	1.10718	1.23311	1.40071
	IHSDT <sup>b</sup>	1.02827	1.11168	1.24257	1.41638
	Reddy's TSDT <sup>a</sup>	1.02766	1.10836	1.23576	1.40556
	Reddy's TSDT <sup>b</sup>	1.02856	1.11283	1.24514	1.42102
	TEHSDT <sup>a</sup>	1.02751	1.10777	1.23444	1.40316
	TEHSDT <sup>b</sup>	1.02841	1.11225	1.24385	1.4187
	Touratier's theory <sup>a</sup>	1.02762	1.10822	1.23543	1.40495
	Touratier's theory <sup>b</sup>	1.02852	1.11269	1.24482	1.42042
10	FSDT [58]	1.0150	1.0590	1.1292	1.2216
	HSDT 7DOF [58]	1.0150	1.0589	1.1290	1.2213
	FEM-ITS DT 7DOF [65]	1.0150	1.0590	1.1289	1.2212
	IHSDT <sup>a</sup>	1.01489	1.05829	1.12841	1.22095
	IHSDT <sup>b</sup>	1.01527	1.05975	1.13255	1.22785
	Reddy's TSDT <sup>a</sup>	1.01497	1.05856	1.12903	1.2220
	Reddy's TSDT <sup>b</sup>	1.01535	1.06003	1.13319	1.22895
	TEHSDT <sup>a</sup>	1.01493	1.05841	1.12869	1.22143
	TEHSDT <sup>b</sup>	1.01531	1.05987	1.13283	1.22833
	Touratier's theory <sup>a</sup>	1.01496	1.05853	1.12897	1.2219
	Touratier's theory <sup>b</sup>	1.01534	1.06000	1.13312	1.22883
20	FSDT [58]	1.01170	1.0460	1.1011	1.1742
	HSDT 7DOF [58]	1.01170	1.0460	1.1010	1.1741
	FEM-ITS DT 7DOF [65]	1.01170	1.0459	1.1009	1.1739
	IHSDT <sup>a</sup>	1.01164	1.04576	1.10081	1.1739
	IHSDT <sup>b</sup>	1.01176	1.04623	1.10214	1.17615
	Reddy's TSDT <sup>a</sup>	1.01166	1.04585	1.10099	1.1742
	Reddy's TSDT <sup>b</sup>	1.01178	1.04631	1.10233	1.17647
	TEHSDT <sup>a</sup>	1.01165	1.0458	1.10088	1.17402
	TEHSDT <sup>b</sup>	1.01177	1.04626	1.10221	1.17627
	Touratier's theory <sup>a</sup>	1.01166	1.04584	1.10097	1.17417
	Touratier's theory <sup>b</sup>	1.01178	1.0463	1.10231	1.17643
40	FSDT [58]	1.0108	1.0426	1.0938	1.1619
	HSDT 7DOF [58]	1.0108	1.0426	1.0937	1.1618
	FEM-ITS DT 7DOF [65]	1.0108	1.0425	1.0936	1.1614
	IHSDT <sup>a</sup>	1.01081	1.04257	1.09343	1.1619
	IHSDT <sup>b</sup>	1.01084	1.04269	1.0937	1.16251
	Reddy's TSDT <sup>a</sup>	1.01082	1.04259	1.09348	1.16199
	Reddy's TSDT <sup>b</sup>	1.01085	1.04272	1.09375	1.16261
	TEHSDT <sup>a</sup>	1.01081	1.04258	1.09345	1.16193
	TEHSDT <sup>b</sup>	1.01085	1.04270	1.09372	1.16254
	Touratier's theory <sup>a</sup>	1.01082	1.04259	1.09348	1.16198
	Touratier's theory <sup>b</sup>	1.01085	1.04272	1.09375	1.16259

<sup>a</sup>von Kármán.

<sup>b</sup>Green–Lagrange for different theories.

more accurate one gives less hardening effect [66,67]. Also, as the  $a/h$  ratio increases, these differences get narrowed. Hence, it can be opined that these theories are to be more selective for the analysis of thick or moderately thick plate than the thin plate.

#### 3.4.3. Effect of material anisotropy on nonlinear free vibration of laminated composite plate

The effect of modulus ratio,  $E_1/E_2$  on nonlinear frequency ratio, ( $\bar{\omega}_{nl}/\bar{\omega}_l$ ) of a simply supported (SSSS – 3) square cross-ply ( $0^\circ/90^\circ/0^\circ/90^\circ$ ) laminated plate with  $a/h = 10$  is listed in **Table 5** for various shear deformation theories. The material properties of each lamina are considered as MM2 with  $E_2 = 10^6 \text{ N/cm}^2$ . The frequency ratio increases with an increase in  $E_1/E_2$  and amplitude ratio, which can be observed in **Table 5**. Moreover, from the **Table 5**, it is observed that at a higher value of  $E_1/E_2$ , the increase in the rate of nonlinearity is more as the amplitude ratio increases due to increase in stiffening effect by the both parameters ( $E_1/E_2$  and  $w_{max}/h$ ). In this case also, it is observed that the solution obtained from various theories are in well agreement with the available one, and the IHSDT response is predicting least hardening effect.

**Table 4**

Nonlinear frequency ratio ( $\bar{\omega}_{nl}/\bar{\omega}_l$ ) for a simply supported (SSSS – 3) angle-ply (45°/–45°/45°/–45°)<sub>3</sub> square laminated plate.

a/h	Source/Method	$w_{max}/h$			
		0.1	0.2	0.3	0.4
5	FSDT [58]	1.0283	1.1096	1.2363	–
	HSDT 7DOF [58]	1.0283	1.1098	1.2366	–
	FEM-ITS DT 7DOF [65]	1.0176	1.0686	1.1488	1.2523
	IHS DT <sup>a</sup>	1.01724	1.06717	1.14691	1.25116
	IHS DT <sup>b</sup>	1.01754	1.06846	1.15043	1.25683
	Reddy's TSDT <sup>a</sup>	1.01755	1.06834	1.14936	1.25516
	Reddy's TSDT <sup>b</sup>	1.01789	1.06963	1.15285	1.26075
	TEHSDT <sup>a</sup>	1.01744	1.06793	1.14849	1.25373
	TEHSDT <sup>b</sup>	1.01778	1.06922	1.15199	1.25936
	Touratier's theory <sup>a</sup>	1.01752	1.06824	1.14915	1.25482
10	Touratier's theory <sup>b</sup>	1.01786	1.06953	1.15265	1.26043
	FSDT [58]	1.0152	1.0597	1.1308	1.2242
	HSDT 7DOF [58]	1.0152	1.0597	1.1307	1.2241
	FEM-ITS DT 7DOF [65]	1.0080	1.0315	1.0697	1.1209
	IHS DT <sup>a</sup>	1.00791	1.03127	1.06901	1.1203
	IHS DT <sup>b</sup>	1.00808	1.03193	1.07043	1.12341
	Reddy's TSDT <sup>a</sup>	1.00796	1.03144	1.06938	1.12095
	Reddy's TSDT <sup>b</sup>	1.00813	1.03211	1.07082	1.12409
	TEHSDT <sup>a</sup>	1.00796	1.03146	1.06941	1.12098
	TEHSDT <sup>b</sup>	1.00813	1.03212	1.07084	1.1241
20	Touratier's theory <sup>a</sup>	1.00796	1.03147	1.06943	1.12103
	Touratier's theory <sup>b</sup>	1.00813	1.03213	1.07086	1.12416
	FSDT [58]	1.0118	1.0465	1.1020	1.1758
	HSDT 7DOF [58]	1.0118	1.0465	1.1019	1.1757
	FEM-ITS DT 7DOF [65]	1.0054	1.0215	1.0479	1.0837
	IHS DT <sup>a</sup>	1.00543	1.02155	1.04784	1.08355
	IHS DT <sup>b</sup>	1.00549	1.02178	1.04836	1.08443
	Reddy's TSDT <sup>a</sup>	1.00544	0.02157	1.0479	1.08364
	Reddy's TSDT <sup>b</sup>	1.0055	1.02181	1.04842	1.08454
	TEHSDT <sup>a</sup>	1.00545	1.0216	1.04796	1.08375
40	TEHSDT <sup>b</sup>	1.00551	1.02184	1.04848	1.08463
	Touratier's theory <sup>a</sup>	1.00544	1.02159	1.04793	1.0837
	Touratier's theory <sup>b</sup>	1.0055	1.02183	1.04845	1.08459
	FSDT [58]	1.0109	1.0430	1.0946	1.1631
	HSDT 7DOF [58]	1.0109	1.0430	1.0946	1.1631
	FEM-ITS DT 7DOF [65]	1.0048	1.0189	1.0420	1.0737
	IHS DT <sup>a</sup>	1.00478	1.01899	1.04222	1.07389
	IHS DT <sup>b</sup>	1.0048	1.01905	1.04237	1.07414
	Reddy's TSDT <sup>a</sup>	1.00478	1.01899	1.04223	1.07389
	Reddy's TSDT <sup>b</sup>	1.0048	1.01906	1.04237	1.07415
40	TEHSDT <sup>a</sup>	1.00479	1.01900	1.04226	1.07395
	TEHSDT <sup>b</sup>	1.0048	1.01907	1.0424	1.0742
	Touratier's theory <sup>a</sup>	1.00478	1.01899	1.04224	1.07392
	Touratier's theory <sup>b</sup>	1.0048	1.01906	1.04239	1.07417

<sup>a</sup>von Kármán.<sup>b</sup>Green–Lagrange for different theories.

### 3.5. Transient analysis

In this section, the linear and geometrically nonlinear transient analysis of laminated composite plate is extensively studied using inverse hyperbolic shear deformation theory (IHS DT). For the geometric nonlinearity, both von Kármán and Green–Lagrange strain–displacement relations have been considered, which address the coupling between bending and membrane behavior. A comparative study has been carried out between linear and nonlinear solution to draw the need for considering full geometric nonlinearity into the formulation. The consideration of nonlinearity makes the structural stiffness higher, which in turn decreases the magnitude of deflection with respect to linear solution. The nonlinear set of governing equations has been solved by considering the nonlinear Newmark algorithm along with the Newton–Raphson method. The time step used for the Newmark scheme varies problem to problem in the present work. The initial estimation of the time step for nonlinear analysis is done by following the process given by Tsui and Tong [68], and Kant and Kommineni [69], in which, they

**Table 5**

Nonlinear frequency ratio ( $\bar{\omega}_{nl}/\bar{\omega}_l$ ) for a simply supported (SSSS – 3) cross-ply (0°/90°/90°/0°) square laminated plate with  $a/h = 10$ .

$E_1/E_2$	Source/Method	$w_{max}/h$			
		0.1	0.2	0.3	0.5
3	FEM-ITS DT 7DOF [65]	1.0075	1.0297	1.0658	1.1747
	IHS DT <sup>a</sup>	1.00751	1.02970	1.06563	1.17482
	IHS DT <sup>b</sup>	1.00791	1.03128	1.06907	1.18649
	Reddy's TSDT <sup>a</sup>	1.00751	1.02972	1.06568	1.17496
	Reddy's TSDT <sup>b</sup>	1.00792	1.03131	1.06915	1.18672
	TEHSDT <sup>a</sup>	1.00751	1.02971	1.06566	1.1749
	TEHSDT <sup>b</sup>	1.00792	1.03129	1.0691	1.18658
	Touratier's theory <sup>a</sup>	1.00751	1.02972	1.06568	1.11478
	Touratier's theory <sup>b</sup>	1.00792	1.03131	1.06914	1.18669
	FEM-ITS DT 7DOF [65]	1.0105	1.0416	1.0916	1.2392
10	IHS DT <sup>a</sup>	1.01051	1.04139	1.09086	1.24002
	IHS DT <sup>b</sup>	1.01094	1.04306	1.09446	1.25200
	Reddy's TSDT <sup>a</sup>	1.01053	1.04147	1.09104	1.24044
	Reddy's TSDT <sup>b</sup>	1.01097	1.04316	1.09467	1.25251
	TEHSDT <sup>a</sup>	1.01052	1.04143	1.09096	1.24026
	TEHSDT <sup>b</sup>	1.01095	1.04311	1.09457	1.25226
	Touratier's theory <sup>a</sup>	1.01053	1.04147	1.09103	1.24043
	Touratier's theory <sup>b</sup>	1.01096	1.04315	1.09465	1.25248
	FEM-ITS DT 7DOF [65]	1.0128	1.0506	1.1112	1.2882
	IHS DT <sup>a</sup>	1.01279	1.05021	1.11083	1.28924
20	IHS DT <sup>b</sup>	1.01321	1.05183	1.11542	1.30055
	Reddy's TSDT <sup>a</sup>	1.01284	1.05038	1.1112	1.29003
	Reddy's TSDT <sup>b</sup>	1.01326	1.05201	1.11582	1.30142
	TEHSDT <sup>a</sup>	1.01282	1.0503	1.11103	1.28969
	TEHSDT <sup>b</sup>	1.01324	1.05192	1.11563	1.30101
	Touratier's theory <sup>a</sup>	1.01283	1.05037	1.11118	1.29002
	Touratier's theory <sup>b</sup>	1.01326	1.05200	1.11579	1.30138
	FEM-ITS DT 7DOF [65]	1.0147	1.0577	1.1262	1.3246
	IHS DT <sup>a</sup>	1.01457	1.05705	1.12588	1.32766
	IHS DT <sup>b</sup>	1.01497	1.05859	1.13022	1.33822
30	Reddy's TSDT <sup>a</sup>	1.01464	1.05731	1.1264	1.32871
	Reddy's TSDT <sup>b</sup>	1.01504	1.05887	1.13078	1.33934
	TEHSDT <sup>a</sup>	1.01461	1.05719	1.12617	1.32828
	TEHSDT <sup>b</sup>	1.01501	1.05873	1.13051	1.33884
	Touratier's theory <sup>a</sup>	1.01464	1.05729	1.12638	1.32872
	Touratier's theory <sup>b</sup>	1.01504	1.05884	1.13075	1.33932
	FEM-ITS DT 7DOF [65]	1.0163	1.0640	1.1397	1.3584
	IHS DT <sup>a</sup>	1.01618	1.06319	1.13941	1.36235
	IHS DT <sup>b</sup>	1.01656	1.06466	1.14353	1.37224
	Reddy's TSDT <sup>a</sup>	1.01626	1.06352	1.14006	1.36356
40	Reddy's TSDT <sup>b</sup>	1.01665	1.06501	1.14422	1.37352
	TEHSDT <sup>a</sup>	1.01622	1.06336	1.13977	1.36308
	TEHSDT <sup>b</sup>	1.01661	1.06484	1.14389	1.37298
	Touratier's theory <sup>a</sup>	1.01626	1.0635	1.14004	1.3636
	Touratier's theory <sup>b</sup>	1.01664	1.06498	1.14418	1.37353

<sup>a</sup>von Kármán.<sup>b</sup>Green–Lagrange for different theories.

suggested:

$$\Delta t \leq \Delta t_{cr} = \Delta x \left\{ \frac{\rho(1 - \nu^2)/E_2}{\{2 + (1 - \nu)(\pi^2/12)(1 + 1.5(\Delta x/h)^2)\}} \right\}^{1/2} \quad (31)$$

where  $\Delta x$  is the smallest distance between adjacent nodes in any employed quadrilateral element. However, to get the final estimation of time step, a convergence study has been carried out.

Further, in the first part of this section, an orthotropic plate and a cross-ply laminated composite plate are considered for the analysis which are accompanied by the validation of the present nonlinear results with the available solution along with presentation of some novel results. In the second part, an angle-ply laminated composite plate is taken for the analysis. The results have been again validated with the available solution and several new results have been presented for the various type of applied load. In the last and third part, damped transient responses have been obtained for the linear and von Kármán nonlinearity. A phase portrait study has also been done in this section.

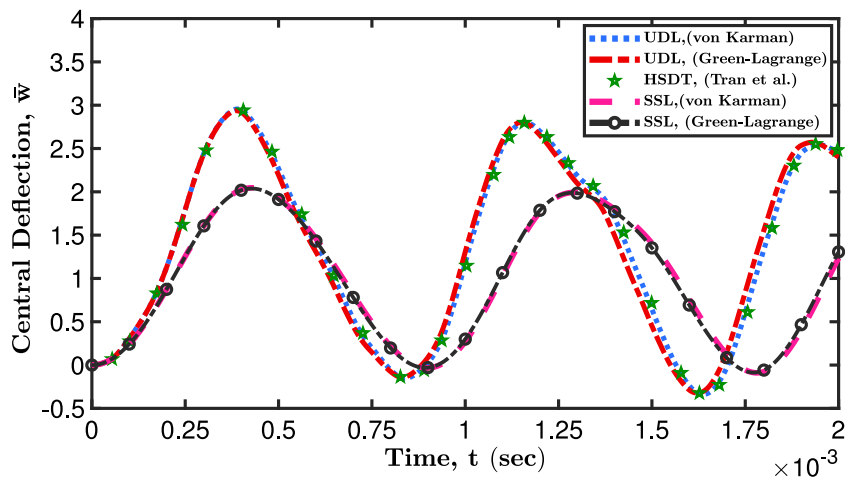


Fig. 2. Time history of the transverse displacement of an orthotropic plate under uniform step load with intensity 1 MPa.

### 3.5.1. Transient analysis of orthotropic plate

To carry out the validation of the present method, a nonlinear transient analysis is performed for an orthotropic plate. The orthotropic plate has a square dimension of length,  $a = 250$  mm, and thickness,  $h = 5$  mm. It is made of material *MM3*. The uniformly distributed load (UDL) and sinusoidally distributed load (SSL) with intensity 1 MPa in conjunction with the time-dependent step load are applied for time,  $t_1 = 2$  ms. The time-step,  $\Delta t = 10^{-5}$  s is considered for the transient response under simply supported (*SSSS-1*) boundary condition. The response is obtained for the von Kármán and Green–Lagrange sense of nonlinearity.

The obtained transient response of normalized central deflection, ( $\bar{w} = w/h$ ) for an orthotropic plate is shown in the Fig. 2. It is observed in the figure that the obtained response for von Kármán is in conformity with the available solution of Tran et al. [59]. The Fig. 2 also presents the response for Green–Lagrange nonlinearity, which is one of the novel work for the present paper, as there is no literature available for the orthotropic plate utilizing the nonpolynomial shear deformation theory with the consideration of full geometric nonlinearity. The von Kármán and Green–Lagrange responses are almost the same, with little increase in frequency for the Green–Lagrange strain. The present transient response provides a standard solution for the orthotropic plate utilizing the nonpolynomial shear deformation theory.

### 3.5.2. Four-layered laminated composite plate under SSL and UDL

To carry out the validation of the present method for the laminated composite plate, a nonlinear transient analysis is performed for four-layered cross-ply [ $0^\circ/90^\circ/90^\circ/0^\circ$ ] and angle-ply [ $45^\circ/-45^\circ/45^\circ/-45^\circ$ ] laminated composite plates under *SSSS-1* boundary condition and the obtained solutions are presented in Fig. 3. The plate has a square dimension of length,  $a = 250$  mm, and thickness,  $h = 5$  mm. It is also made of material *MM3*. The uniformly distributed load (UDL) and sinusoidally distributed load (SSL) with intensity 1 MPa in conjunction with the time-dependent step load are applied for  $t_1 = 2$  ms. The time-step,  $\Delta t = 1 \times 10^{-6}$  s is considered for the transient response calculation. The response of normalized central deflection,  $\bar{w}$  is obtained for the von Kármán and Green–Lagrange sense of nonlinearity and shown in Figs. 3a and 3b. The present transient responses of normalized central deflection,  $\bar{w}$  under time-dependent step load for UDL has been compared with the available result of Chen et al. [60] and found to be in well agreement. Further, the transient responses of cross-ply [ $0^\circ/90^\circ/90^\circ/0^\circ$ ] and angle-ply [ $45^\circ/-45^\circ/45^\circ/-45^\circ$ ] for sinusoidal load have also been obtained and shown in Figs. 3c and 3d. It is observed from these plots that for this particular problem the difference between von Kármán and Green–Lagrange is not significant due to less transverse deflection magnitude.

### 3.5.3. Three-layered cross-ply laminated plate under various types of loads

A three-layered cross-ply [ $0^\circ/90^\circ/0^\circ$ ] laminated composite plate under simply supported (*SSSS-1*) boundary condition is considered for the transient analysis employing various dynamic loads. The plate is made of material *MM4* and each individual layers are of equal thickness with  $h = 0.1526$  m. A sinusoidal distributed load (SSL) of magnitude 0.689 GPa is applied for the analysis of a laminated plate with side-to-thickness ratio,  $a/h = 5$ . A step pulse load is applied for  $t_1 = 6$  ms and  $t_1 = 5$  ms; and the responses are obtained and shown in Fig. 4. It is observed in the Figs. 4a and 4b that the pattern of deflection response for free vibration is found to be different for different time of loading. This is due to the dependence of transient response on the initial conditions. The amplitude of free vibration seems to depend on the amplitude of vibration at the time of removing the applied force. Since each response has different amplitude at the time of removal of applied load, each response follow a different pattern for the free vibration.

Moreover, various types of load, namely step, sinusoidal, exponential, and triangular load are applied for 5 ms and the response is obtained for 10 ms. The responses are shown in Fig. 5 for the von Kármán (Fig. 5a) and Green–Lagrange (Fig. 5b) strain. Here, it is observed that in the free vibration response, when load is removed, the structure is vibrating with the same natural frequency, which suggests that the free vibration response frequency is not affected by the applied excitation load, however, the amplitude of vibration in the free vibration range, not only depends on the type of load applied but also on the time till which load is being applied.

Now, the same problem is analyzed for the various time-dependent loads, namely step, sinusoidal, exponential, and triangular load applied for  $t_1 = 3$  ms, and the obtained responses are shown in Fig. 6. The response is obtained for the von Kármán and Green–Lagrange strain along with the linear solution for a sinusoidally distributed transverse load. Further, the response for various dynamic load such as step load (Fig. 6a), sinusoidal load (Fig. 6b), exponential load (Fig. 6c), and triangular load (Fig. 6d) also signify the need for nonlinear analysis as the differences in the response become quite significant for some specific type of loads.

### 3.5.4. Three-layered cross-ply laminated composite plate under various boundary conditions

In this section, the transient response for various boundary conditions have been obtained for different magnitude of the load. The obtained responses for various boundary conditions, namely *SSSS-1*, *SSSS-3*, *SSSS-4*, *CCCC*, *SSFS*, *CCFC* are shown in the Fig. 7. The boundary condition notation, such as ‘*ABCD*’, represents ‘*A*’ at  $y = 0$ , ‘*B*’ at  $y = b$ , ‘*C*’ at  $x = a$ , and ‘*D*’ at  $x = 0$ . The sinusoidally

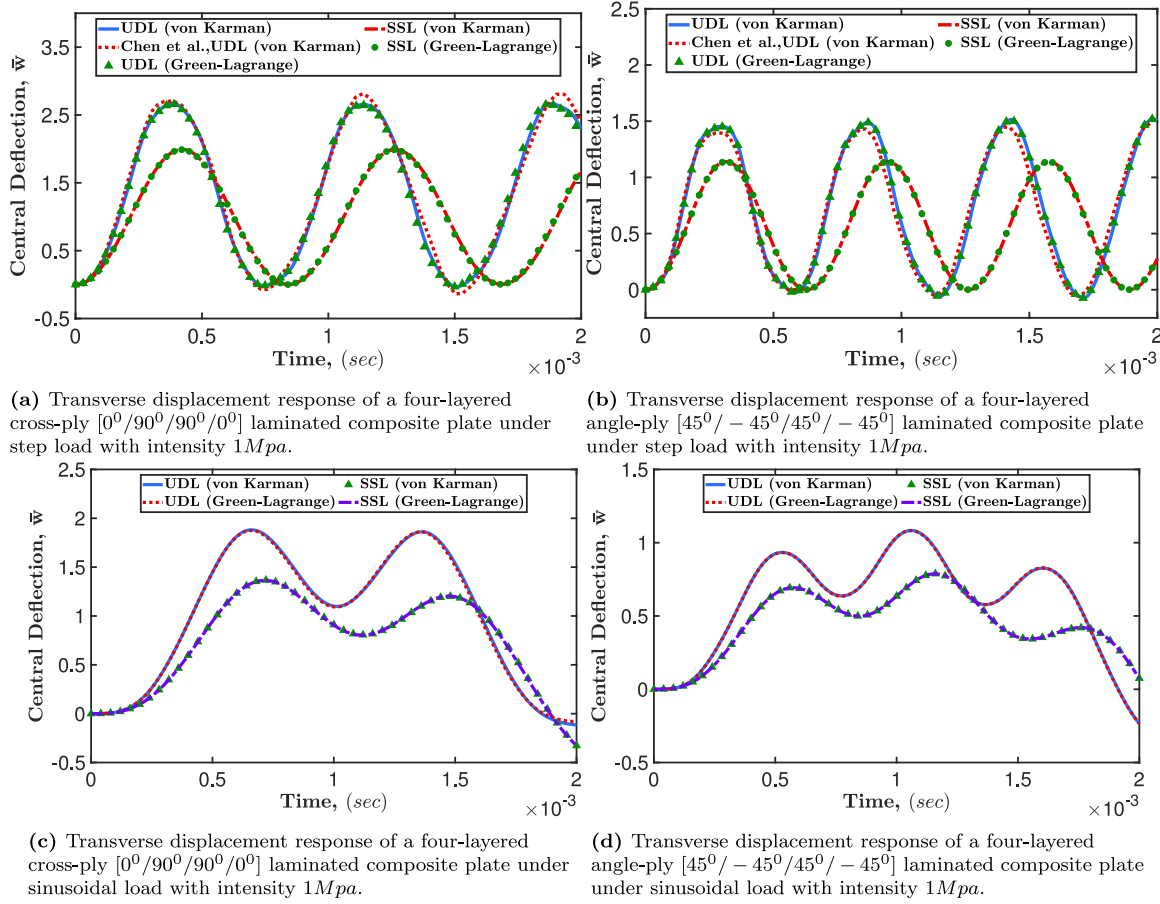


**Fig. 3.** Transient transverse displacement response of four-layered laminated composite plate under uniformly distributed load (UDL) and sinusoidal distribution load (SSL) for  $SSSS-1$  boundary condition.

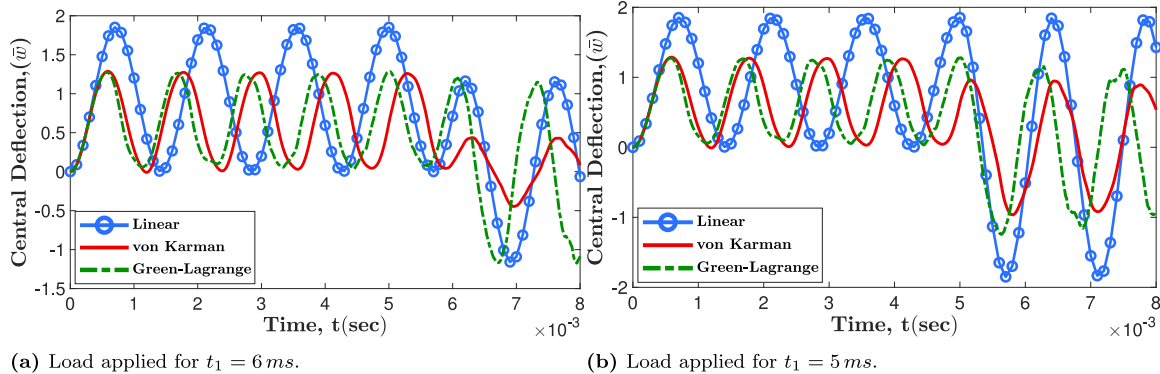


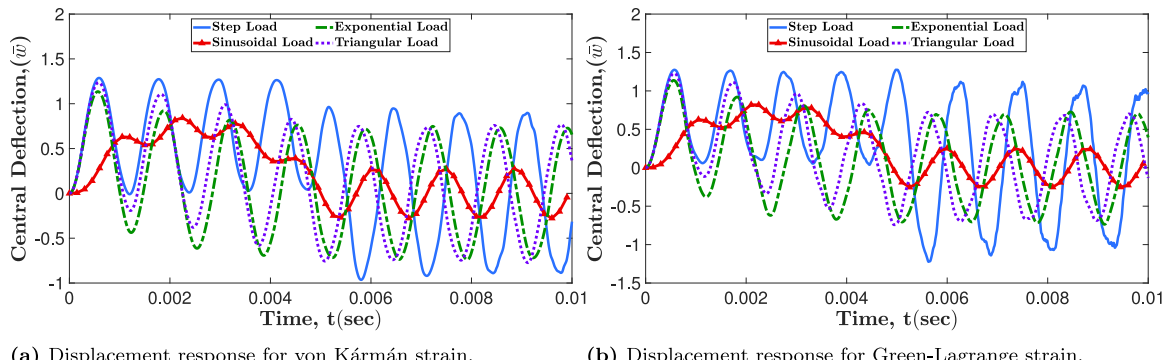
**Fig. 4.** Transient response of the transverse displacement of square laminated [0°/90°/0°] composite plate under sinusoidal step load applied for  $t_1 = 6$  ms and  $t_1 = 5$  ms.

distributed loads with magnitude  $P$ ,  $0.8P$ ,  $0.6P$ , where  $P = 0.689$  GPa, are applied for  $t_1 = 5$  ms. It is observed in the Fig. 7 that the variation in the response of von Kármán and Green-Lagrange solution are highly affected by the consideration of boundary condition. In the case of  $SSSS-1$  as shown in Fig. 7a, the significant difference is observed at the loads  $0.8P$  and  $0.6P$ ; whereas in the case of  $SSSS-3$  (Fig. 7b),  $SSSS-4$  (Fig. 7c), and  $CCFC$  (Fig. 7d), not much difference is observed even at the applied load of  $P$  and  $0.8P$ . On the other hand, a significant difference is observed between von Kármán and Green-Lagrange response at the low magnitude load ( $0.8P$ , and  $0.6P$ ) and ( $P$ , and  $0.8P$ ) for the  $SSFS$  (Fig. 7e) and  $CCFC$  (Fig. 7f) boundary conditions, respectively. The more constrained boundary condition generates more stiffening effect, and as the constraints of the boundary

reduces from clamped to simply supported to free boundary condition, the frequency decreases and deflection amplitude increases. This is why, a significant difference is observed in the response of  $CCFC$  and  $SSFS$  boundary condition with respect to other boundary conditions for the stated load. These observations are of immense importance to analyze the structure under various boundary conditions.

### 3.5.5. Damping analysis of laminated composite plate

A cross-ply [0°/90°/90°/0°] laminated composite plate is considered for the damped transient analysis, which considers the Rayleigh damping model to incorporate the damping in the system. The plate is made of material  $MM5$  and has side-length of  $a = b = 25$  cm, and side-to-thickness ratio,  $a/h = 10$ . The transverse step load along with



(a) Displacement response for von Kármán strain.

(b) Displacement response for Green-Lagrange strain.

**Fig. 5.** Transient response of the transverse displacement of square laminated  $[0^\circ/90^\circ/0^\circ]$  composite plate under various time-dependent load and sinusoidally distributed spatial load applied for  $t_1 = 5$  ms under the consideration of von Kármán and Green-Lagrange strains.

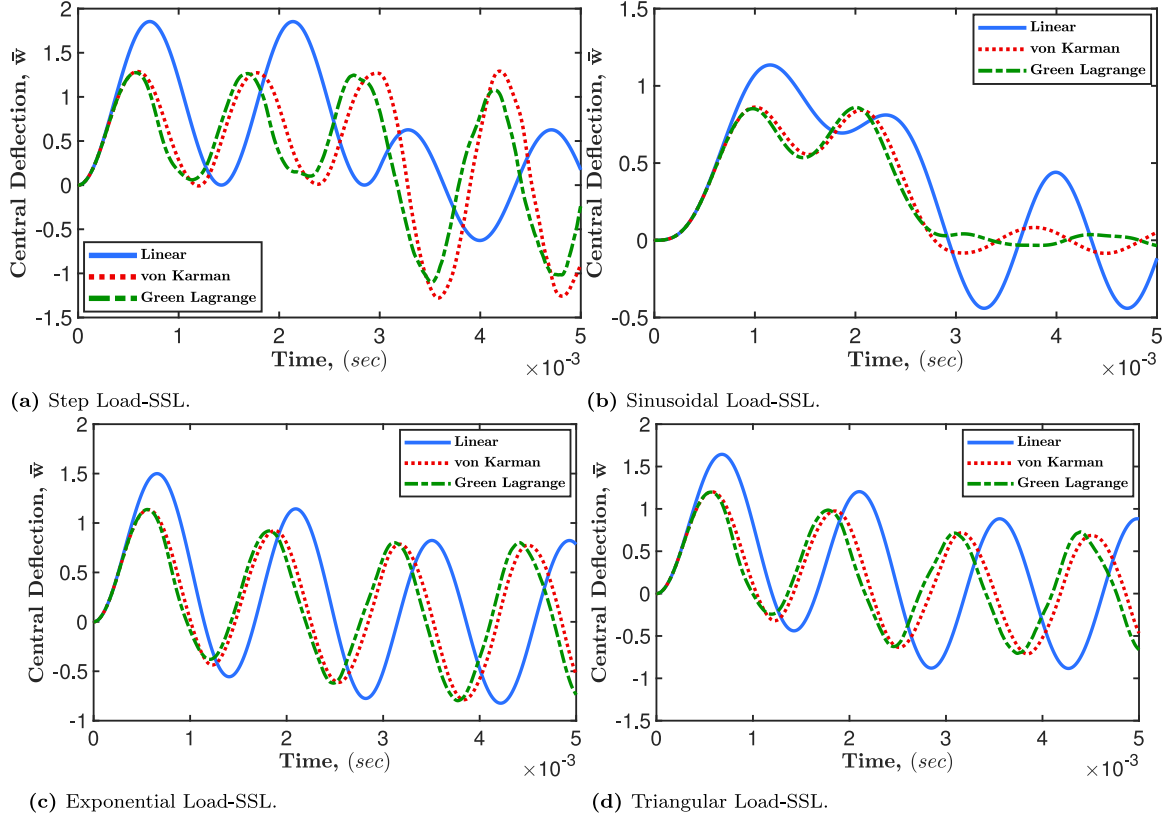


**Fig. 6.** Transient response of  $[0^\circ/90^\circ/0^\circ]$  laminated composite plate under various blast loads corresponding to sinusoidal distribution load (SSL) for  $SSSS-1$  boundary condition.

uniformly distributed load (UDL) is applied for the time  $t_1 = 1.6$  ms, and the time-step taken for the analysis is  $\Delta t = 10^{-5}$  s. The analysis is carried out for applied nondimensional load,  $Q = (q_0 b^4)/(E_2 h^4) = 10$ , under uniformly distributed step load and simply supported,  $SSSS-1$  boundary condition. To validate the present approach for the damping analysis, a linear solution is obtained, and the result is validated by the available solution of Latheswary et al. [42]. The obtained response is shown in the Fig. 8a. It is observed from the figure that the present solution is in good agreement with the available solution.

Further, the Rayleigh damping coefficients are obtained by considering the first two modes of vibration for the damping ratio,  $\xi = 1\%$  and  $5\%$ . The same Rayleigh damping coefficients are employed to obtain the damped response for the von Kármán sense of nonlinearity. The damped responses for the linear and von Kármán nonlinearity for uniformly distributed step load are shown in the Fig. 8b. These responses are obtained by employing the step load of magnitude of

nondimensional load,  $Q = (q_0 b^4)/(E_2 h^4) = 100$  for  $t_1 = 1.6$  ms. The responses shown in Fig. 8b are for the damping ratio,  $\xi = 1\%$  and  $5\%$ .

Moreover, a phase plot with the derivative of transverse displacement against the transverse displacement are also shown in Fig. 9. It gives the phase plot for linear and von Kármán sense of strain for the damping ratio,  $\xi = 0\%$ ,  $\xi = 1\%$ , and  $\xi = 5\%$  under sinusoidally distributed and uniformly distributed load. From the phase portrait plot Fig. 9, it is observed that the undamped solution produces neutrally stable solution whereas damped response provides an asymptotically stable solution which tends to zero velocity over time. Moreover, it also reveals that the linear damped/undamped solution covers bigger range of transverse displacement than the nonlinear damped/undamped solution whereas the range of velocity remains almost same. These are the insightful information which can be obtained by observing the phase plot, which signify such plot for the pragmatic analysis of dynamic problems.

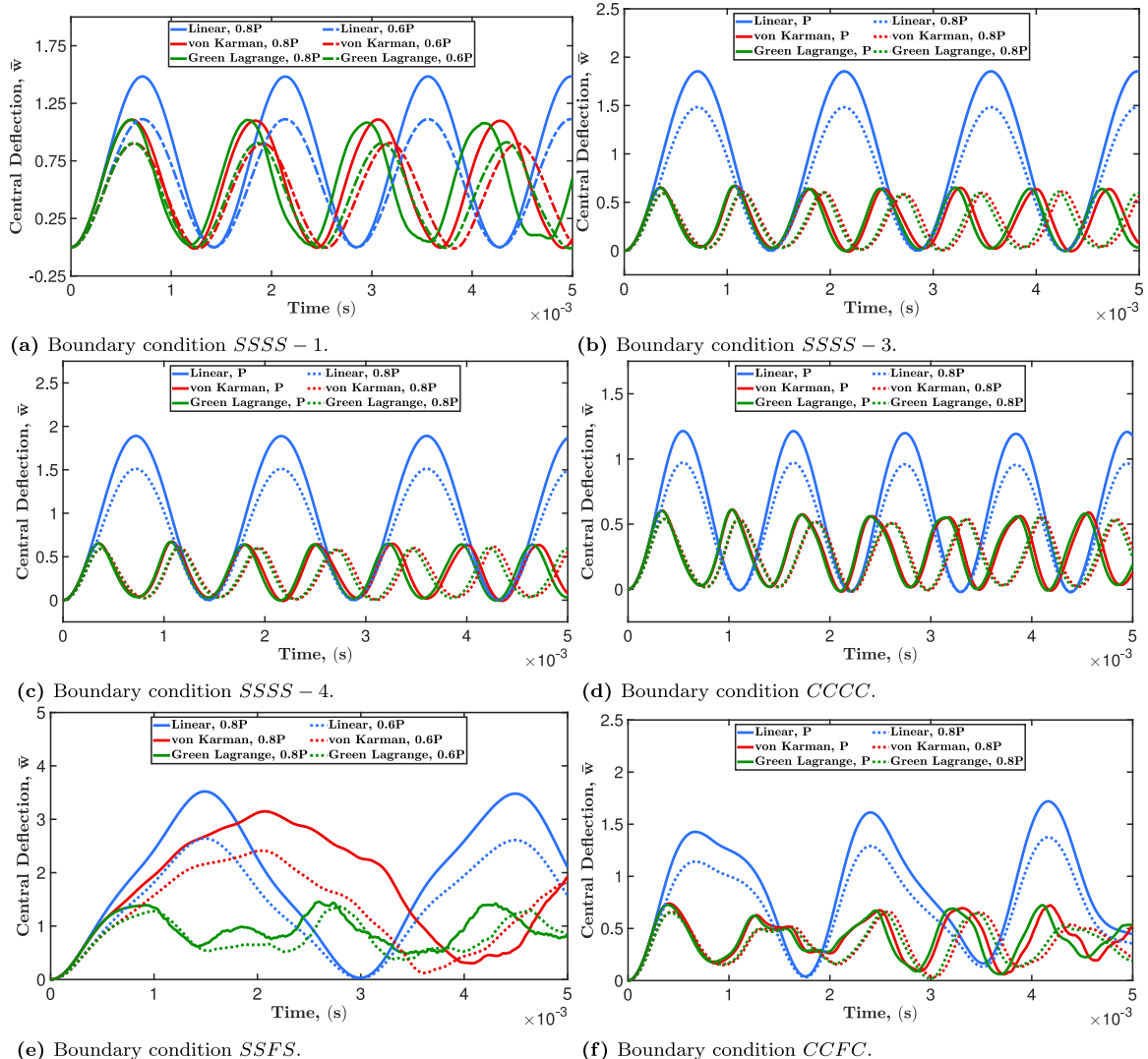


**Fig. 7.** Transient response of  $[0^\circ/90^\circ/0^\circ]$  laminated composite plate under various loading magnitude corresponding to sinusoidal distributed step load for different boundary conditions.

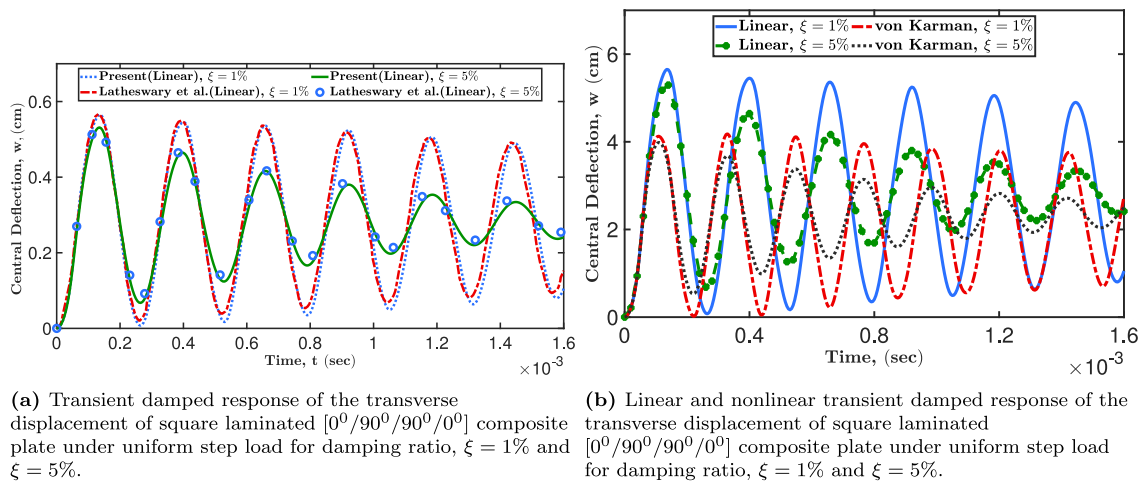


**Fig. 8.** Transient damped transverse displacement response of laminated composite  $[0^\circ/90^\circ/90^\circ/0^\circ]$  plate under uniform distribution load (UDL) for  $SSSS - 1$  boundary condition.

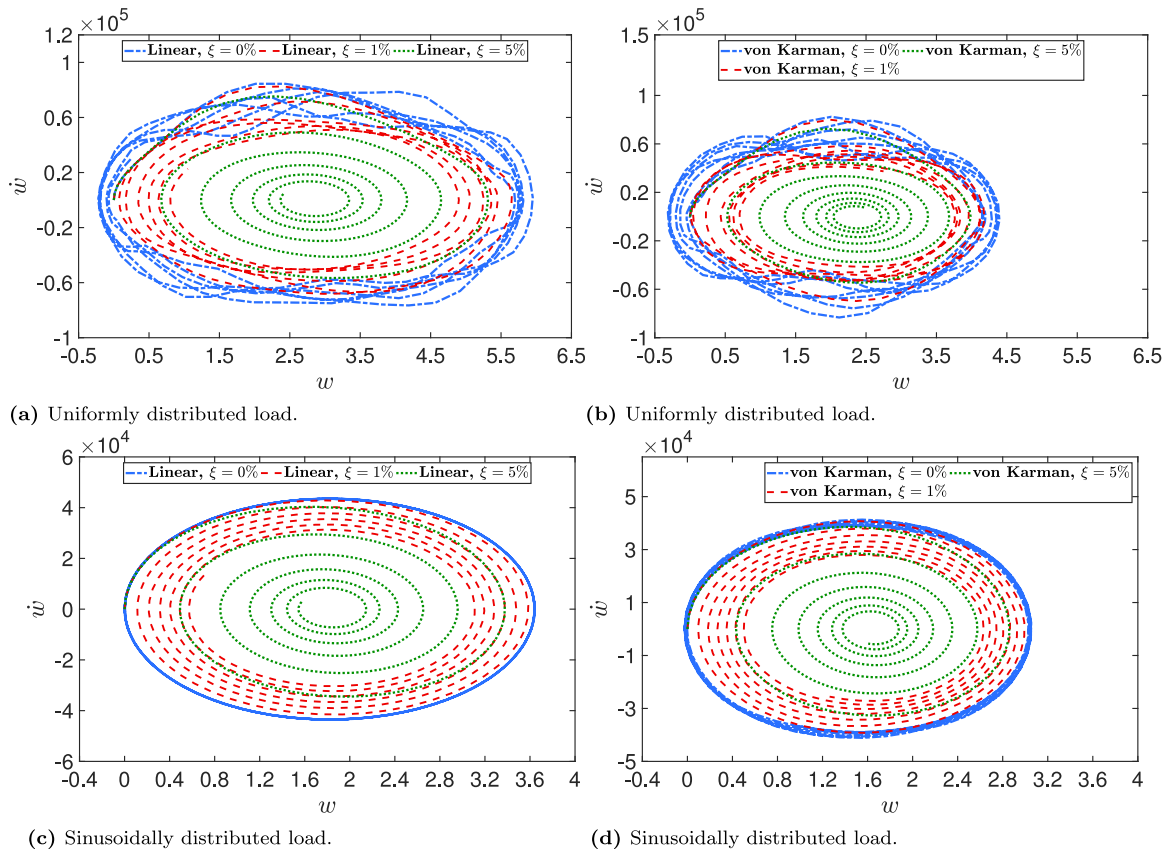
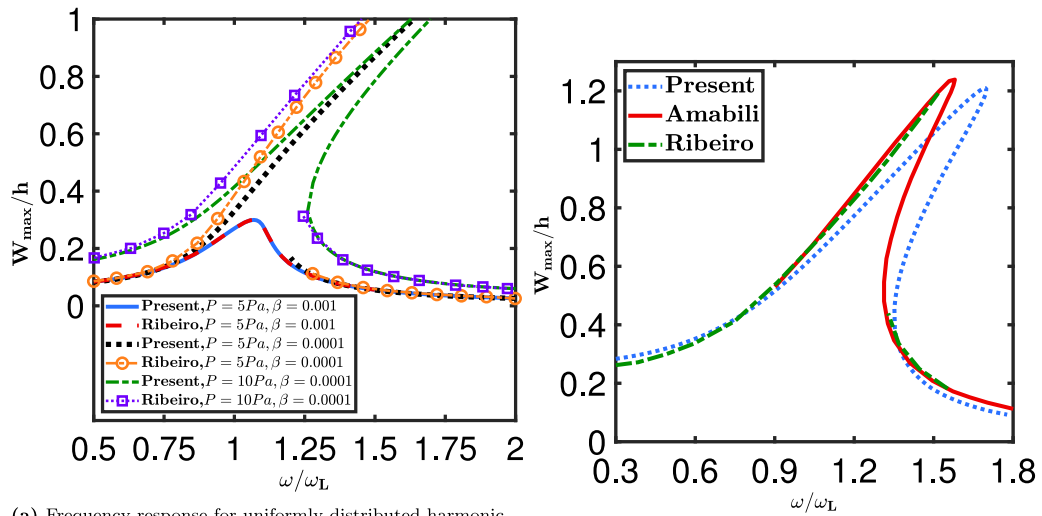


Fig. 9. Phase plot of  $[0^\circ/90^\circ/0^\circ]$  laminated composite plate under uniform distribution load (UDL) and sinusoidal distribution load (SSL) for  $SSSS - 1$  boundary condition.



(a) Frequency response for uniformly distributed harmonic load with various load magnitude and damping ratio,  $\beta = 0.1\%$  and  $\beta = 0.01\%$ .

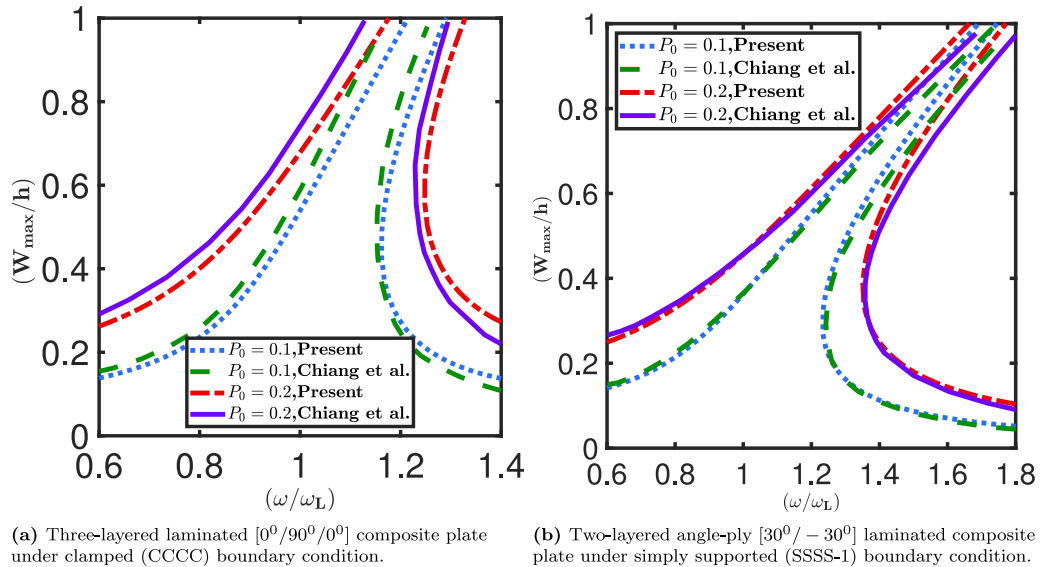
(b) Frequency response for central point load of magnitude  $P = 1.74$  N with damping coefficient  $\alpha = 0.065$ .

Fig. 10. First harmonic frequency response of Aluminum plate under immovable simply supported (SSSS-3) boundary condition.

### 3.6. Steady state forced vibration analysis

In this section, the nonlinear steady-state solution in the frequency domain has been analyzed for various plate structures by applying the harmonic force with excitation frequency around the natural frequency. Only IHSDT has been considered for the harmonic analysis, as it is found to be performing well for the nonlinear free vibration in the previous section. Further, the von Kármán nonlinearity has been considered for the incorporation of geometric nonlinearity as

it is observed that Green–Lagrange does not provide any significant change for thin plate. For the sake of brevity, to obtain the harmonic response, only one harmonic, i.e.,  $\{q\} = \{A\}\cos(\omega t) + \{B\}\sin(\omega t)$  has been considered. The arc-length continuation method has been applied to obtained the response [44]. The frequency response shows the plot of central nondimensional displacement ( $W_{max}/h$ ) and frequency ratio ( $\omega/\omega_L$ ), where  $W_{max}$  is the transverse deflection obtained from  $\{W_{max}\} = \sqrt{\{A\}\cdot\{A\} + \{B\}\cdot\{B\}}$ ,  $\omega$  is the forcing frequency, and  $\omega_L$  is the fundamental natural frequency.



**Fig. 11.** Frequency response of three-layered cross-ply [0°/90°/0°] and two-layered angle-ply [30°/-30°] laminated composite plates subjected to uniformly distributed load under simply supported (SSSS-1) and clamped (CCCC) boundary conditions, respectively, with no damping consideration.

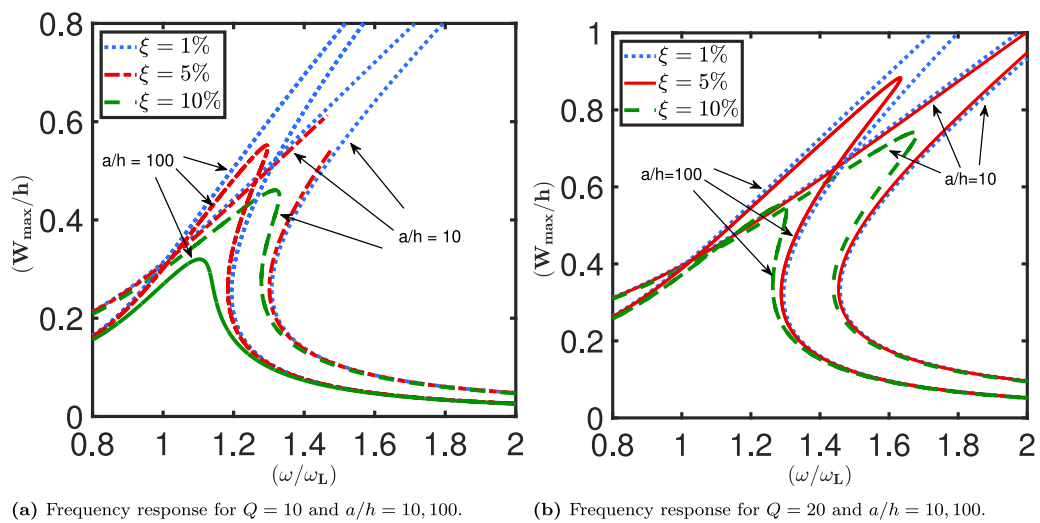


**Fig. 12.** Frequency response of four-layered laminated composite [0°/90°/90°/0°] plate under simply supported (SSSS-1) boundary condition.

### 3.6.1. Frequency response of Aluminum plate

To validate the present formulation for the harmonic analysis, an isotropic Aluminum plate is considered with dimensions:  $a = 0.6$  m,  $b = 0.3$  m,  $h = 0.001$  m. The material properties for the same are as follows:  $E = 70$  GPa,  $\nu = 0.3$ ,  $\rho = 2778$  kg/m<sup>3</sup> [66,70]. The immovable simply supported (SSSS-3) boundary condition is considered with uniformly distributed harmonic force excitation,  $P = P_0 \cos(\omega t)$ , where  $P_0$  is the excitation amplitude and  $\omega$  is the excitation frequency. For the incorporation of damping,  $\alpha = 0$ ,  $\beta = 10^{-3}, 10^{-4}$  are considered.

The frequency response is obtained for various,  $P_0$  and damping coefficient,  $\beta$  and shown in Fig. 10a. It can be observed that the present solution is in good agreement with the available solution of Ribeiro [70] for  $\beta = 10^{-3}$ , albeit with some discrepancies for  $\beta = 10^{-4}$ . It is observed that due to approximation of field variable with single harmonic in the present analysis, the obtained results deviate from the higher harmonic numerical solution when the vibration frequency approaches the fundamental natural frequency.

Further, one more plate with the material properties as mentioned above is considered for the steady state forced vibration analysis. The plate having dimensions  $a = 0.3$  m,  $b = 0.3$  m and  $h = 0.001$  m is subjected to concentrated harmonic excitation force of magnitude  $P_0 = 1.74$  N at the center of the plate. The obtained frequency response is shown in Fig. 10b. Again, it is observed that, due to consideration of only one harmonic to approximate the field variable, the present response shows some discrepancies at higher displacement amplitude as compared by the analytical solution of Amabili [66] and third harmonic solution of Ribeiro [71].

### 3.6.2. Frequency response of a laminated composite plate without damping

In this section, the steady-state solution is obtained for square laminated plate under clamped (CCCC) and simply supported (SSSS-1) boundary conditions. The plate with dimensions,  $a = b = 0.3048$  m, and  $a/h = 100$  m, and material properties:  $E_1 = 40E_2$ ,  $E_2 = 5.171$  GPa,  $G_{12} = G_{13} = 0.5E_2$ ,  $G_{23} = 0.2E_2$ ,  $\nu_{12} = 0.25$ ,  $\rho = 2564.856$  kg/m<sup>3</sup> [72], is

$$\begin{aligned}
A_b \phi_b = & \left[ \begin{array}{cccccccccccccc} 
\frac{\partial u_0}{\partial x} & \frac{\partial v_0}{\partial x} & \frac{\partial w_0}{\partial x} & 0 & 0 & 0 & 0 & 0 & 0 & 0 & 0 & 0 & 0 & 0 & 0 & 0 \\
0 & 0 & 0 & \frac{\partial u_0}{\partial y} & \frac{\partial v_0}{\partial y} & \frac{\partial w_0}{\partial y} & 0 & 0 & 0 & 0 & 0 & 0 & 0 & 0 & 0 & 0 \\
\frac{\partial u_0}{\partial y} & \frac{\partial v_0}{\partial y} & \frac{\partial w_0}{\partial y} & \frac{\partial u_0}{\partial x} & \frac{\partial v_0}{\partial x} & \frac{\partial w_0}{\partial x} & 0 & 0 & 0 & 0 & 0 & 0 & 0 & 0 & 0 & 0 \\
\frac{\partial \phi_x}{\partial x} & \frac{\partial \phi_y}{\partial x} & 0 & 0 & 0 & 0 & \frac{\partial u_0}{\partial x} & 0 & \frac{\partial v_0}{\partial x} & 0 & 0 & 0 & 0 & 0 & 0 & 0 \\
0 & 0 & 0 & \frac{\partial \phi_x}{\partial y} & \frac{\partial \phi_y}{\partial y} & 0 & 0 & \frac{\partial u_0}{\partial y} & 0 & \frac{\partial v_0}{\partial y} & 0 & 0 & 0 & 0 & 0 & 0 \\
\frac{\partial \phi_x}{\partial y} & \frac{\partial \phi_y}{\partial y} & 0 & \frac{\partial \phi_x}{\partial x} & \frac{\partial \phi_y}{\partial x} & 0 & \frac{\partial u_0}{\partial y} & \frac{\partial v_0}{\partial x} & \frac{\partial w_0}{\partial y} & 0 & 0 & 0 & 0 & 0 & 0 & 0 \\
\frac{\partial \theta_x}{\partial x} & \frac{\partial \theta_y}{\partial x} & 0 & 0 & 0 & 0 & 0 & 0 & 0 & 0 & \frac{\partial u_0}{\partial x} & 0 & \frac{\partial v_0}{\partial x} & 0 & 0 & 0 \\
0 & 0 & 0 & \frac{\partial \theta_x}{\partial y} & \frac{\partial \theta_y}{\partial y} & 0 & 0 & 0 & 0 & 0 & \frac{\partial u_0}{\partial y} & 0 & \frac{\partial v_0}{\partial y} & 0 & 0 & 0 \\
\frac{\partial \theta_x}{\partial y} & \frac{\partial \theta_y}{\partial y} & 0 & \frac{\partial \theta_x}{\partial x} & \frac{\partial \theta_y}{\partial x} & 0 & 0 & 0 & 0 & 0 & \frac{\partial u_0}{\partial y} & \frac{\partial v_0}{\partial x} & 0 & \frac{\partial w_0}{\partial y} & 0 \\
0 & 0 & 0 & 0 & 0 & 0 & \frac{\partial \theta_x}{\partial x} & 0 & \frac{\partial \theta_y}{\partial x} & 0 & 0 & \frac{\partial \phi_x}{\partial x} & 0 & \frac{\partial \phi_y}{\partial x} & 0 & 0 \\
0 & 0 & 0 & 0 & 0 & 0 & 0 & \frac{\partial \theta_x}{\partial y} & 0 & \frac{\partial \theta_y}{\partial y} & 0 & 0 & \frac{\partial \phi_x}{\partial y} & 0 & \frac{\partial \phi_y}{\partial y} & 0 \\
0 & 0 & 0 & 0 & 0 & 0 & \frac{\partial \theta_x}{\partial y} & \frac{\partial \theta_y}{\partial x} & \frac{\partial \theta_y}{\partial y} & 0 & \frac{\partial \phi_x}{\partial x} & \frac{\partial \phi_y}{\partial y} & 0 & \frac{\partial \phi_y}{\partial x} & 0 \\
0 & 0 & 0 & 0 & 0 & 0 & \frac{\partial \theta_x}{\partial x} & 0 & \frac{\partial \theta_y}{\partial x} & 0 & 0 & \frac{\partial \phi_x}{\partial x} & 0 & \frac{\partial \phi_y}{\partial x} & 0 \\
0 & 0 & 0 & 0 & 0 & 0 & 0 & \frac{\partial \theta_x}{\partial y} & 0 & \frac{\partial \theta_y}{\partial y} & 0 & 0 & \frac{\partial \phi_x}{\partial y} & 0 & \frac{\partial \phi_y}{\partial y} & 0 \\
0 & 0 & 0 & 0 & 0 & 0 & 0 & \frac{\partial \theta_x}{\partial y} & \frac{\partial \theta_y}{\partial x} & \frac{\partial \theta_y}{\partial y} & 0 & \frac{\partial \phi_x}{\partial y} & \frac{\partial \phi_y}{\partial x} & 0 & \frac{\partial \phi_y}{\partial y} & 0 \\
0 & 0 & 0 & 0 & 0 & 0 & 0 & 0 & 0 & 0 & \frac{\partial \theta_x}{\partial x} & 0 & \frac{\partial \theta_y}{\partial x} & 0 & 0 & 0 \\
0 & 0 & 0 & 0 & 0 & 0 & 0 & 0 & 0 & 0 & \frac{\partial \theta_x}{\partial y} & 0 & \frac{\partial \theta_y}{\partial y} & 0 & 0 & 0 \\
0 & 0 & 0 & 0 & 0 & 0 & 0 & 0 & 0 & 0 & \frac{\partial \theta_x}{\partial y} & \frac{\partial \theta_y}{\partial x} & \frac{\partial \theta_y}{\partial y} & 0 & \frac{\partial \theta_x}{\partial x} & 0 \\
\end{array} \right] \quad \left\{ \begin{array}{l} \frac{\partial u_0}{\partial x} \\ \frac{\partial v_0}{\partial x} \\ \frac{\partial w_0}{\partial x} \\ \frac{\partial \phi_x}{\partial x} \\ \frac{\partial \phi_y}{\partial x} \\ \frac{\partial \theta_x}{\partial x} \\ \frac{\partial \theta_y}{\partial x} \\ \frac{\partial \phi_x}{\partial y} \\ \frac{\partial \phi_y}{\partial y} \\ \frac{\partial \theta_x}{\partial y} \\ \frac{\partial \theta_y}{\partial y} \\ \frac{\partial \phi_x}{\partial y} \\ \frac{\partial \phi_y}{\partial y} \\ \frac{\partial \theta_x}{\partial y} \\ \frac{\partial \theta_y}{\partial x} \\ \frac{\partial \theta_y}{\partial y} \\ \frac{\partial \phi_x}{\partial y} \\ \frac{\partial \phi_y}{\partial x} \\ \frac{\partial \theta_x}{\partial x} \\ \frac{\partial \theta_y}{\partial x} \\ \frac{\partial \theta_x}{\partial y} \\ \frac{\partial \theta_y}{\partial y} \\ \frac{\partial \theta_x}{\partial y} \\ \frac{\partial \theta_y}{\partial x} \end{array} \right\} \\
\\
A_s \phi_s = & \left[ \begin{array}{cccccccccccccc} 
0 & \phi_x & 0 & \phi_y & 0 & 0 & 0 & 0 & 0 & 0 & 0 & 0 & 0 & 0 & 0 & 0 \\
\phi_x & 0 & \phi_y & 0 & 0 & 0 & 0 & 0 & 0 & 0 & 0 & 0 & 0 & 0 & 0 & 0 \\
0 & 0 & 0 & 0 & 0 & \phi_x & 0 & \phi_y & 0 & 0 & 0 & 0 & 0 & 0 & 0 & 0 \\
0 & 0 & 0 & 0 & 0 & \phi_x & 0 & \phi_y & 0 & 0 & 0 & 0 & 0 & 0 & 0 & 0 \\
0 & 0 & 0 & 0 & 0 & 0 & 0 & 0 & 0 & \phi_x & 0 & \phi_y & 0 & 0 & 0 & 0 \\
0 & 0 & 0 & 0 & 0 & 0 & 0 & 0 & 0 & 0 & 0 & \phi_x & 0 & \phi_y & 0 & 0 \\
0 & 0 & 0 & 0 & 0 & 0 & 0 & 0 & 0 & 0 & 0 & \phi_x & 0 & \phi_y & 0 & 0 \\
0 & \theta_x & 0 & \theta_y & 0 & 0 & 0 & 0 & 0 & 0 & 0 & 0 & 0 & 0 & 0 & 0 \\
\theta_x & 0 & \theta_y & 0 & 0 & 0 & 0 & 0 & 0 & 0 & 0 & 0 & 0 & 0 & 0 & 0 \\
0 & 0 & 0 & 0 & 0 & \theta_x & 0 & \theta_y & 0 & 0 & 0 & 0 & 0 & 0 & 0 \\
0 & 0 & 0 & 0 & 0 & \theta_x & 0 & \theta_y & 0 & 0 & 0 & 0 & 0 & 0 & 0 \\
0 & 0 & 0 & 0 & 0 & 0 & 0 & 0 & \theta_x & 0 & \theta_y & 0 & 0 & 0 & 0 & 0 \\
0 & 0 & 0 & 0 & 0 & 0 & 0 & 0 & \theta_x & 0 & \theta_y & 0 & 0 & 0 & 0 & 0 \\
\end{array} \right] \quad \left\{ \begin{array}{l} \frac{\partial u_0}{\partial x} \\ \frac{\partial v_0}{\partial x} \\ \frac{\partial w_0}{\partial x} \\ \frac{\partial \phi_x}{\partial x} \\ \frac{\partial \phi_y}{\partial x} \\ \frac{\partial \theta_x}{\partial x} \\ \frac{\partial \theta_y}{\partial x} \\ \frac{\partial \phi_x}{\partial y} \\ \frac{\partial \phi_y}{\partial y} \\ \frac{\partial \theta_x}{\partial y} \\ \frac{\partial \theta_y}{\partial y} \\ \frac{\partial \phi_x}{\partial y} \\ \frac{\partial \phi_y}{\partial y} \\ \frac{\partial \theta_x}{\partial x} \\ \frac{\partial \theta_y}{\partial x} \\ \frac{\partial \theta_x}{\partial y} \\ \frac{\partial \theta_y}{\partial x} \\ \frac{\partial \theta_x}{\partial x} \\ \frac{\partial \theta_y}{\partial x} \\ \frac{\partial \theta_x}{\partial y} \\ \frac{\partial \theta_y}{\partial x} \\ \frac{\partial \theta_x}{\partial x} \\ \frac{\partial \theta_y}{\partial x} \end{array} \right\}
\end{aligned}$$

Box II.

considered. A harmonic force with excitation frequency in the neighborhood of natural frequency is applied for the analysis. The magnitude of the applied force is nondimensionalized as  $P_0 = cP/\rho h^2 \omega_l^2$ , where  $P$  is the actual force applied,  $\omega_l$  is the linear frequency. The constant  $c$  is given by expression  $c = \iint \phi dx dy / \iint \phi^2 dx dy$ , which is the ratio of volume under mode shape and square of mode shape as mentioned by Chiang et al. [72]. The harmonic responses without any damping consideration are obtained for clamped (CCCC) and simply supported (SSSS-1) boundary conditions employing nondimensional force,  $P_0 = 0.1$  and 0.2, and the obtained responses are shown in Figs. 11a and 11b, respectively. It is observed that the present solutions are in good agreement with little discrepancies with the solution of Chiang et al. [72]. This difference can be attributed to the consideration of IHSDT in the present formulation as CLPT has been used with the modal reduction to single mode by the Chiang et al. [72]. Moreover, these solutions provide a good agreement for the validation of the present formulation considering single harmonic approximation.

### 3.6.3. Frequency response of a four-layered cross-ply laminated composite plate

In this section, the harmonic analysis is carried out for the problem analyzed previously in Section 3.5.5 for  $a/h = 10$  and  $a/h = 100$ . The frequency response is obtained for nondimensional load,  $Q = (q_0 b^4) / (E_2 h^4) = 10, 20$  under simply supported (SSSS-1) boundary condition and shown in Fig. 12. It is observed that for  $a/h = 10$ , the responses for  $\xi = 1\%$  and  $5\%$  are almost same, while for the  $a/h = 100$ , all three responses are significantly different due to thin plate. From the Fig. 12, it is also observed that the thick plate ( $a/h = 10$ ) provides more hardening effect than the thin plate. It should be noted that for the sake of brevity, these results have been obtained by considering only one harmonic approximation of field variables, as a result, some error could be found in the solution when the frequency of vibration approaches fundamental natural frequency. Besides, to obtain the more accurate solution, one needs to consider higher harmonic approximation, as evident from the previous examples. However, the present solution

$$S_b = \begin{bmatrix} N_x & 0 & 0 & N_{xy} & 0 & 0 & M_x & M_{xy} & 0 & 0 & P_x & P_{xy} & 0 & 0 \\ 0 & N_x & 0 & 0 & N_{xy} & 0 & 0 & 0 & M_x & M_{xy} & 0 & 0 & P_x & P_{xy} \\ 0 & 0 & N_x & 0 & 0 & N_{xy} & 0 & 0 & 0 & 0 & 0 & 0 & 0 & 0 \\ N_{xy} & 0 & 0 & N_y & 0 & 0 & M_{xy} & M_y & 0 & 0 & P_{xy} & P_y & 0 & 0 \\ 0 & N_{xy} & 0 & 0 & N_y & 0 & 0 & 0 & M_{xy} & M_y & 0 & 0 & P_{xy} & P_y \\ 0 & 0 & N_{xy} & 0 & 0 & N_y & 0 & 0 & 0 & 0 & 0 & 0 & 0 & 0 \\ M_x & 0 & 0 & M_{xy} & 0 & 0 & L_x & L_{xy} & 0 & 0 & R_x & R_{xy} & 0 & 0 \\ M_{xy} & 0 & 0 & M_y & 0 & 0 & L_{xy} & L_y & 0 & 0 & R_{xy} & R_y & 0 & 0 \\ 0 & M_x & 0 & 0 & M_{xy} & 0 & 0 & 0 & L_x & L_{xy} & 0 & 0 & R_x & R_{xy} \\ 0 & M_{xy} & 0 & 0 & M_y & 0 & 0 & 0 & L_{xy} & L_y & 0 & 0 & R_{xy} & R_y \\ P_x & 0 & 0 & P_{xy} & 0 & 0 & R_x & R_{xy} & 0 & 0 & V_x & V_{xy} & 0 & 0 \\ P_{xy} & 0 & 0 & P_y & 0 & 0 & R_{xy} & R_y & 0 & 0 & V_{xy} & V_y & 0 & 0 \\ 0 & P_x & 0 & 0 & P_{xy} & 0 & 0 & 0 & R_x & R_{xy} & 0 & 0 & V_x & V_{xy} \\ 0 & P_{xy} & 0 & 0 & P_y & 0 & 0 & 0 & R_{xy} & R_y & 0 & 0 & V_{xy} & V_y \end{bmatrix}$$
  

$$S_s = \begin{bmatrix} 0 & 0 & 0 & 0 & 0 & 0 & 0 & 0 & 0 & 0 & 0 & N_{xz} & 0 & R_{xz} & 0 \\ 0 & 0 & 0 & 0 & 0 & 0 & 0 & 0 & 0 & 0 & 0 & N_{yz} & 0 & R_{yz} & 0 \\ 0 & 0 & 0 & 0 & 0 & 0 & 0 & 0 & 0 & 0 & 0 & 0 & 0 & N_{xz} & 0 & R_{xz} \\ 0 & 0 & 0 & 0 & 0 & 0 & 0 & 0 & 0 & 0 & 0 & 0 & 0 & N_{yz} & 0 & R_{yz} \\ 0 & 0 & 0 & 0 & 0 & 0 & 0 & 0 & 0 & 0 & 0 & 0 & 0 & M_{xz} & 0 & L_{xz} \\ 0 & 0 & 0 & 0 & 0 & 0 & 0 & 0 & 0 & 0 & 0 & 0 & 0 & M_{yz} & 0 & L_{yz} \\ 0 & 0 & 0 & 0 & 0 & 0 & 0 & 0 & 0 & 0 & 0 & 0 & 0 & 0 & M_{xz} & 0 & L_{xz} \\ 0 & 0 & 0 & 0 & 0 & 0 & 0 & 0 & 0 & 0 & 0 & 0 & 0 & 0 & M_{yz} & 0 & L_{yz} \\ 0 & 0 & 0 & 0 & 0 & 0 & 0 & 0 & 0 & 0 & 0 & 0 & 0 & P_{xz} & 0 & V_{xz} \\ 0 & 0 & 0 & 0 & 0 & 0 & 0 & 0 & 0 & 0 & 0 & 0 & 0 & P_{yz} & 0 & V_{yz} \\ 0 & 0 & 0 & 0 & 0 & 0 & 0 & 0 & 0 & 0 & 0 & 0 & 0 & P_{xz} & 0 & V_{xz} \\ 0 & 0 & 0 & 0 & 0 & 0 & 0 & 0 & 0 & 0 & 0 & 0 & 0 & P_{yz} & 0 & V_{yz} \\ N_{xz} & N_{yz} & 0 & 0 & M_{xz} & M_{yz} & 0 & 0 & P_{xz} & P_{yz} & 0 & 0 & 0 & 0 & 0 & 0 \\ 0 & 0 & N_{xz} & N_{yz} & 0 & 0 & M_{xz} & M_{yz} & 0 & 0 & P_{xz} & P_{yz} & 0 & 0 & 0 & 0 \\ R_{xz} & R_{yz} & 0 & 0 & L_{xz} & L_{yz} & 0 & 0 & V_{xz} & V_{yz} & 0 & 0 & 0 & 0 & 0 & 0 \\ 0 & 0 & R_{xz} & R_{yz} & 0 & 0 & L_{xz} & L_{yz} & 0 & 0 & V_{xz} & V_{yz} & 0 & 0 & 0 & 0 \end{bmatrix}$$

## Box III.

provides a standard finite element solution for higher-order theories with first harmonic approximation.

#### 4. Conclusion

Geometrically nonlinear free vibration, transient, and steady-state forced vibration analysis of laminated composite plate are extensively carried out utilizing inverse hyperbolic shear deformation theory. The inclusion of geometric nonlinearity is done through the incorporation of von Kármán and Green–Lagrange strain–displacement relations. In the first part, nonlinear free vibration has been analyzed for von Kármán and Green–Lagrange sense of strains. The nonlinear frequency ratios for various side-to-thickness ratios, material anisotropy ratios, and lamination scheme have been evaluated. The difference between von Kármán and Green–Lagrange results are found to be significant due to von Kármán being an approximation of Green–Lagrange nonlinearity, and hence, it emphasizes the need for consideration of full geometric nonlinearity. Moreover, the present nonlinear free vibration analysis provides a standard benchmark solution for the laminated composite plate utilizing nonpolynomial shear deformation theory with full geometric nonlinearity, as there is a lack of availability of the same in the literature. In the second part, the present work deals with the transient analysis of laminated composite plate. The displacement–time response has been obtained for various dynamic loading, namely step, sinusoidal, triangular, and exponential load for various boundary conditions. The paper provides a comprehensive comparative study among linear, von Kármán, and Green–Lagrange sense of nonlinearity. It is observed from the transient response that the consideration of nonlinearity is entangled with several other factors such as the boundary conditions, material properties, and the applied load, as the differences observed

for the different parameters vary significantly. Moreover, damped transient analysis has also been presented using Rayleigh damping model. The damped model is firstly validated by linear analysis, and the Rayleigh damping coefficients are obtained from the linear analysis, and the same Rayleigh damping coefficients are used in the calculation of damped response for von Kármán sense of nonlinearity. A phase portraits for the damped transient analysis have also been shown to properly visualize the variation of central velocity and central deflection of the plate. As this kind of work has not been addressed in the available literature; hence, the present work provides a novel and reliable solution to ponder upon for the further nonlinear analysis on the nonpolynomial higher-order shear deformation theory. This seminal work presents a standard solution for the geometric nonlinear dynamic analysis of laminated composite plate utilizing inverse hyperbolic shear deformation theory. Overall, the present study emphasizes the scope and the requirements of full geometric nonlinearity consideration in the dynamic structural analysis.

#### CRediT authorship contribution statement

**Babu Ranjan Thakur:** Conceptualization, Methodology, Data curation, Visualization, Writing - original draft, Programming. **Surendra Verma:** Conceptualization, Methodology, Visualization, Writing - original draft, Programming. **B.N. Singh:** Conceptualization, Supervision, Reviewing and editing. **D.K. Maiti:** Conceptualization, Supervision, Reviewing and editing.

#### Declaration of competing interest

The authors declare that they have no known competing financial interests or personal relationships that could have appeared to influence the work reported in this paper.

## Appendix A. The expression for $A_b\phi_b$ and $A_s\phi_s$

$A_b\phi_b$ ,  $A_s\phi_s$  are given in Box II.

## Appendix B. The resulting in-plane and shear stresses

$$\begin{aligned} & \begin{bmatrix} N_{xx} & M_{xx} & P_{xx} & R_{xx} & L_{xx} & V_{xx} \\ N_{yy} & M_{yy} & P_{yy} & R_{yy} & L_{yy} & V_{yy} \\ N_{xy} & M_{xy} & P_{xy} & R_{xy} & L_{xy} & V_{xy} \end{bmatrix} \\ & = \int_{-\frac{h}{2}}^{\frac{h}{2}} \left\{ \begin{array}{c} \sigma_{xx} \\ \sigma_{yy} \\ \tau_{xy} \end{array} \right\} \{1 \quad z \quad f(z) \quad zf(z) \quad z^2 \quad f^2(z)\} dz \\ \\ & \begin{bmatrix} N_{yz} & M_{yz} & P_{yz} & R_{yz} & L_{yz} & V_{yz} \\ N_{xz} & M_{xz} & P_{xz} & R_{xz} & L_{xz} & V_{xz} \end{bmatrix} \\ & = \int_{-\frac{h}{2}}^{\frac{h}{2}} \left\{ \begin{array}{c} \tau_{yz} \\ \tau_{xz} \end{array} \right\} \{1 \quad z \quad f(z) \quad f'(z) \quad zf'(z) \quad f(z)f'(z)\} dz \end{aligned}$$

## Appendix C. The expression of $B_{bli}$ , $B_{sli}$ , $G_{bnli}$ , and $G_{snli}$

$$\begin{aligned} B_{bli} &= \begin{bmatrix} \frac{\partial N_i}{\partial x} & 0 & 0 & 0 & 0 & 0 & 0 \\ 0 & \frac{\partial N_i}{\partial y} & 0 & 0 & 0 & 0 & 0 \\ \frac{\partial N_i}{\partial y} & 0 & 0 & 0 & 0 & 0 & 0 \\ 0 & 0 & 0 & \frac{\partial N_i}{\partial x} & 0 & 0 & 0 \\ 0 & 0 & 0 & 0 & \frac{\partial N_i}{\partial y} & 0 & 0 \\ 0 & 0 & 0 & 0 & 0 & \frac{\partial N_i}{\partial x} & 0 \\ 0 & 0 & 0 & 0 & 0 & 0 & \frac{\partial N_i}{\partial y} \end{bmatrix} \\ B_{sli} &= \begin{bmatrix} 0 & 0 & \frac{\partial N_i}{\partial y} & 0 & N_i & 0 & 0 \\ 0 & 0 & \frac{\partial N_i}{\partial x} & N_i & 0 & 0 & 0 \\ 0 & 0 & 0 & 0 & 0 & 0 & N_i \\ 0 & 0 & 0 & 0 & 0 & N_i & 0 \end{bmatrix} \\ G_{bnli} &= \begin{bmatrix} \frac{\partial N_i}{\partial x} & 0 & 0 & 0 & 0 & 0 & 0 \\ 0 & \frac{\partial N_i}{\partial y} & 0 & 0 & 0 & 0 & 0 \\ 0 & 0 & \frac{\partial N_i}{\partial x} & 0 & 0 & 0 & 0 \\ \frac{\partial N_i}{\partial y} & 0 & 0 & 0 & 0 & 0 & 0 \\ 0 & \frac{\partial N_i}{\partial x} & 0 & 0 & 0 & 0 & 0 \\ 0 & 0 & \frac{\partial N_i}{\partial y} & 0 & 0 & 0 & 0 \\ 0 & 0 & 0 & \frac{\partial N_i}{\partial x} & 0 & 0 & 0 \\ 0 & 0 & 0 & 0 & \frac{\partial N_i}{\partial y} & 0 & 0 \\ 0 & 0 & 0 & 0 & 0 & \frac{\partial N_i}{\partial x} & 0 \\ 0 & 0 & 0 & 0 & 0 & 0 & \frac{\partial N_i}{\partial y} \end{bmatrix} \end{aligned}$$

$$G_{snli} = \begin{bmatrix} \frac{\partial N_i}{\partial x} & 0 & 0 & 0 & 0 & 0 & 0 \\ \frac{\partial N_i}{\partial y} & 0 & 0 & 0 & 0 & 0 & 0 \\ 0 & \frac{\partial N_i}{\partial x} & 0 & 0 & 0 & 0 & 0 \\ 0 & \frac{\partial N_i}{\partial y} & 0 & 0 & 0 & 0 & 0 \\ 0 & 0 & 0 & \frac{\partial N_i}{\partial x} & 0 & 0 & 0 \\ 0 & 0 & 0 & \frac{\partial N_i}{\partial y} & 0 & 0 & 0 \\ 0 & 0 & 0 & 0 & \frac{\partial N_i}{\partial x} & 0 & 0 \\ 0 & 0 & 0 & 0 & \frac{\partial N_i}{\partial y} & 0 & 0 \\ 0 & 0 & 0 & 0 & 0 & \frac{\partial N_i}{\partial x} & 0 \\ 0 & 0 & 0 & 0 & 0 & 0 & \frac{\partial N_i}{\partial y} \\ 0 & 0 & 0 & 0 & 0 & N_i & 0 \\ 0 & 0 & 0 & 0 & 0 & 0 & N_i \\ 0 & 0 & 0 & 0 & 0 & 0 & N_i \end{bmatrix}$$

## Appendix D. The expression of $S_b$ and $S_s$

$S_b, S_s$  are given in Box III.

## References

- [1] G. Kirchhoff, Ueber die schwingungen einer kreisförmigen elastischen scheibe, Ann. Phys. 157 (10) (1850) 258–264, <http://dx.doi.org/10.1002/andp.18501571005>.
- [2] E. Reissner, The effect of transverse shear deformation on the bending of elastic plates, 1945.
- [3] R. Mindlin, Influence of rotatory inertia and shear on flexural motions of isotropic, elastic plates, J. Appl. Mech. 18 (1951) 31, [http://dx.doi.org/10.1007/978-1-4613-8865-4\\_29](http://dx.doi.org/10.1007/978-1-4613-8865-4_29).
- [4] P.F. Pai, A new look at shear correction factors and warping functions of anisotropic laminates, Int. J. Solids Struct. 32 (16) (1995) 2295–2313, [http://dx.doi.org/10.1016/0020-7683\(94\)00258-x](http://dx.doi.org/10.1016/0020-7683(94)00258-x).
- [5] A. Bhimaraddi, L. Stevens, A higher order theory for free vibration of orthotropic, homogeneous, and laminated rectangular plates, J. Appl. Mech. 51 (1984) 195, <http://dx.doi.org/10.1115/1.3167569>.
- [6] J.N. Reddy, A simple higher-order theory for laminated composite plates, J. Appl. Mech. 51 (4) (1984) 745–752, <http://dx.doi.org/10.1115/1.3167719>.
- [7] J. Ren, A new theory of laminated plate, Compos. Sci. Technol. 26 (3) (1986) 225–239, [http://dx.doi.org/10.1016/0266-3538\(86\)90087-4](http://dx.doi.org/10.1016/0266-3538(86)90087-4).
- [8] T. Kant, B. Pandya, A simple finite element formulation of a higher-order theory for unsymmetrically laminated composite plates, Compos. Struct. 9 (3) (1988) 215–246, [http://dx.doi.org/10.1016/0263-8223\(88\)90015-3](http://dx.doi.org/10.1016/0263-8223(88)90015-3).
- [9] P.R. Mohan, B. Naganarayana, G. Prathap, Consistent and variationally correct finite elements for higher-order laminated plate theory, Compos. Struct. 29 (4) (1994) 445–456, [http://dx.doi.org/10.1016/0263-8223\(94\)90113-9](http://dx.doi.org/10.1016/0263-8223(94)90113-9).
- [10] M. Touratier, An efficient standard plate theory, Int. J. Eng. Sci. 29 (8) (1991) 901–916, [http://dx.doi.org/10.1016/0020-7222\(91\)90165-y](http://dx.doi.org/10.1016/0020-7222(91)90165-y).
- [11] M. Aydogdu, A new shear deformation theory for laminated composite plates, Compos. Struct. 89 (1) (2009) 94–101, <http://dx.doi.org/10.1016/j.compstruct.2008.07.008>.
- [12] M. Karama, K. Afaq, S. Mistou, A new theory for laminated composite plates, Proc. Inst. Mech. Eng., Part L: J. Mater.: Des. Appl. 223 (2) (2009) 53–62, <http://dx.doi.org/10.1243/14644207jmda189>.
- [13] N. El Meiche, A. Tounsi, N. Ziane, I. Mechab, et al., A new hyperbolic shear deformation theory for buckling and vibration of functionally graded sandwich plate, Int. J. Mech. Sci. 53 (4) (2011) 237–247, <http://dx.doi.org/10.1016/j.ijmecsci.2011.01.004>.
- [14] J. Mantari, A. Oktem, C.G. Soares, A new higher order shear deformation theory for sandwich and composite laminated plates, Composites B 43 (3) (2012) 1489–1499, <http://dx.doi.org/10.1201/b12726-46>.
- [15] J. Mantari, A. Oktem, C.G. Soares, A new trigonometric shear deformation theory for isotropic, laminated composite and sandwich plates, Int. J. Solids Struct. 49 (1) (2012) 43–53, <http://dx.doi.org/10.1016/j.ijsolstr.2011.09.008>.
- [16] N. Grover, B. Singh, D. Maiti, New nonpolynomial shear-deformation theories for structural behavior of laminated-composite and sandwich plates, AIAA J. 51 (8) (2013) 1861–1871, <http://dx.doi.org/10.2514/1.j052399>.

- [17] N. Grover, B. Singh, D. Maiti, Analytical and finite element modeling of laminated composite and sandwich plates: An assessment of a new shear deformation theory for free vibration response, *Int. J. Mech. Sci.* 67 (2013) 89–99, <http://dx.doi.org/10.1016/j.ijmecsci.2012.12.010>.
- [18] A.S. Sayyad, Flexure of thick orthotropic plates by exponential shear deformation theory, *Latin American Journal of Solids and Structures* 10 (3) (2013) 473–490, <http://dx.doi.org/10.1590/s1679-7825201300030002>.
- [19] S. Abrate, M. Di Sciuva, Equivalent single layer theories for composite and sandwich structures: A review, *Compos. Struct.* 179 (2017) 482–494, <http://dx.doi.org/10.1016/j.compstruct.2017.07.090>.
- [20] M. Kolly, K. Chandrashekara, Non-linear static and dynamic analysis of stiffened laminated plates, *Int. J. Non-Linear Mech.* 32 (1) (1997) 89–101, [http://dx.doi.org/10.1016/s0020-7462\(96\)00016-9](http://dx.doi.org/10.1016/s0020-7462(96)00016-9).
- [21] H. Tanrıöver, E. Şenocak, Large deflection analysis of unsymmetrically laminated composite plates: analytical-numerical type approach, *Int. J. Non-Linear Mech.* 39 (8) (2004) 1385–1392, <http://dx.doi.org/10.1016/j.ijnonlinmec.2004.01.001>.
- [22] M.K. Singha, M. Ganapathi, Large amplitude free flexural vibrations of laminated composite skew plates, *Int. J. Non-Linear Mech.* 39 (10) (2004) 1709–1720, <http://dx.doi.org/10.1016/j.ijnonlinmec.2004.04.003>.
- [23] M. Amabili, Nonlinear vibrations of rectangular plates with different boundary conditions: theory and experiments, *Comput. Struct.* 82 (31–32) (2004) 2587–2605, <http://dx.doi.org/10.1016/j.compstruc.2004.03.077>.
- [24] M. Amabili, Theory and experiments for large-amplitude vibrations of rectangular plates with geometric imperfections, *J. Sound Vib.* 291 (3–5) (2006) 539–565, <http://dx.doi.org/10.1016/j.jsv.2005.06.007>.
- [25] K.-D. Kim, S.-C. Han, S. Suthasupradit, Geometrically non-linear analysis of laminated composite structures using a 4-node co-rotational shell element with enhanced strains, *Int. J. Non-Linear Mech.* 42 (6) (2007) 864–881, <http://dx.doi.org/10.1016/j.ijnonlinmec.2007.03.011>.
- [26] Z. Kazancı, Dynamic response of composite sandwich plates subjected to time-dependent pressure pulses, *Int. J. Non-Linear Mech.* 46 (5) (2011) 807–817, <http://dx.doi.org/10.1016/j.ijnonlinmec.2011.03.011>.
- [27] S. Susler, H.S. Turkmen, Z. Kazancı, The nonlinear dynamic behaviour of tapered laminated plates subjected to blast loading, *Shock Vib.* 19 (6) (2012) 1235–1255, <http://dx.doi.org/10.1155/2012/936412>.
- [28] H. Kurtaran, Geometrically nonlinear transient analysis of thick deep composite curved beams with generalized differential quadrature method, *Compos. Struct.* 128 (2015) 241–250, <http://dx.doi.org/10.1016/j.compstruct.2015.03.060>.
- [29] H. Kurtaran, Large displacement static and transient analysis of functionally graded deep curved beams with generalized differential quadrature method, *Compos. Struct.* 131 (2015) 821–831, <http://dx.doi.org/10.1016/j.compstruct.2015.06.024>.
- [30] A. Naghsh, M. Azhari, Non-linear free vibration analysis of point supported laminated composite skew plates, *Int. J. Non-Linear Mech.* 76 (2015) 64–76, <http://dx.doi.org/10.1016/j.ijnonlinmec.2015.05.008>.
- [31] P. Malekzadeh, Differential quadrature large amplitude free vibration analysis of laminated skew plates based on FSDT, *Compos. Struct.* 83 (2) (2008) 189–200, <http://dx.doi.org/10.1016/j.compstruct.2007.04.007>.
- [32] L. Zhang, W. Liu, K. Liew, Geometrically nonlinear large deformation analysis of triangular CNT-reinforced composite plates, *Int. J. Non-Linear Mech.* 86 (2016) 122–132, <http://dx.doi.org/10.1016/j.ijnonlinmec.2016.08.004>.
- [33] G. Akgün, H. Kurtaran, Geometrically nonlinear transient analysis of laminated composite super-elliptic shell structures with generalized differential quadrature method, *Int. J. Non-Linear Mech.* 105 (2018) 221–241, <http://dx.doi.org/10.1016/j.ijnonlinmec.2018.05.016>.
- [34] N. Jafari, M. Azhari, B. Boroomand, Geometrically nonlinear analysis of time-dependent composite plates using time function optimization, *Int. J. Non-Linear Mech.* 116 (2019) 219–229, <http://dx.doi.org/10.1016/j.ijnonlinmec.2019.07.005>.
- [35] T. Kant, K. Swaminathan, Analytical solutions for free vibration of laminated composite and sandwich plates based on a higher-order refined theory, *Compos. Struct.* 53 (1) (2001) 73–85, [http://dx.doi.org/10.1016/s0263-8223\(00\)00180-x](http://dx.doi.org/10.1016/s0263-8223(00)00180-x).
- [36] F. Aljiani, M. Amabili, Non-linear static bending and forced vibrations of rectangular plates retaining non-linearities in rotations and thickness deformation, *Int. J. Non-linear Mech.* 67 (2014) 394–404, <http://dx.doi.org/10.1016/j.ijnonlinmec.2014.10.003>.
- [37] F. Aljiani, M. Amabili, Effect of thickness deformation on large-amplitude vibrations of functionally graded rectangular plates, *Compos. Struct.* 113 (2014) 89–107, <http://dx.doi.org/10.1016/j.compstruct.2014.03.006>.
- [38] M. Amabili, J. Reddy, The nonlinear, third-order thickness and shear deformation theory for statics and dynamics of laminated composite shells, *Compos. Struct.* (2020) 112265, <http://dx.doi.org/10.1016/j.compstruct.2020.112265>.
- [39] N. Zabarás, T. Pervez, Viscous damping approximation of laminated anisotropic composite plates using the finite element method, *Comput. Methods Appl. Mech. Engrg.* 81 (3) (1990) 291–316, [http://dx.doi.org/10.1016/0045-7825\(90\)90058-t](http://dx.doi.org/10.1016/0045-7825(90)90058-t).
- [40] H.T. Banks, D. Inman, On damping mechanisms in beams, *J. Appl. Mech.* 58 (3) (1991) 716–723, <http://dx.doi.org/10.1115/1.2897253>.
- [41] T. Pervez, N. Zabarás, Transient dynamic and damping analysis of laminated anisotropic plates using a refined plate theory, *Internat. J. Numer. Methods Engrg.* 33 (5) (1992) 1059–1080, <http://dx.doi.org/10.1002/nme.1620330511>.
- [42] S. Latheswary, K. Valsarajan, Y. Sadasiva Rao, Dynamic response of moderately thick composite plates, *J. Sound Vib.* 270 (2004) 417–426, [http://dx.doi.org/10.1016/s0022-460x\(03\)00511-x](http://dx.doi.org/10.1016/s0022-460x(03)00511-x).
- [43] Y. Lei, M.I. Friswell, S. Adhikari, A Galerkin method for distributed systems with non-local damping, *Int. J. Solids Struct.* 43 (11–12) (2006) 3381–3400, <http://dx.doi.org/10.1016/j.ijsolstr.2005.06.058>.
- [44] P. Ribeiro, M. Petyt, Geometrical non-linear, steady state, forced, periodic vibration of plates, part i: model and convergence studies, *J. Sound Vib.* 226 (5) (1999) 955–983, <http://dx.doi.org/10.1006/jsvi.1999.2306>.
- [45] P. Ribeiro, M. Petyt, Geometrical non-linear, steady state, forced, periodic vibration of plates, part II: Stability study and analysis of multi-modal response, *J. Sound Vib.* 226 (5) (1999) 985–1010, <http://dx.doi.org/10.1006/jsvi.1999.2336>.
- [46] L. Azrar, E. Bouteyour, M. Potier-Ferry, Non-linear forced vibrations of plates by an asymptotic-numerical method, *J. Sound Vib.* 252 (4) (2002) 657–674, <http://dx.doi.org/10.1006/jsvi.2002.4049>.
- [47] Z. Kazancı, Z. Mecitoglu, Nonlinear damped vibrations of a laminated composite plate subjected to blast load, *AIAA J.* 44 (9) (2006) 2002–2008, <http://dx.doi.org/10.2514/6.2005-2339>.
- [48] F. Boumédiène, A. Miloudi, J.-M. Cadou, L. Duigou, E. Bouteyour, Nonlinear forced vibration of damped plates by an asymptotic numerical method, *Comput. Struct.* 87 (23–24) (2009) 1508–1515, <http://dx.doi.org/10.1016/j.compstruc.2009.07.005>.
- [49] A. Treviso, B. Van Genuchten, D. Mundo, M. Tournour, Damping in composite materials: Properties and models, *Composites B* 78 (2015) 144–152, <http://dx.doi.org/10.1016/j.compositesb.2015.03.081>.
- [50] M. Amabili, F. Aljiani, J. Delannoy, Damping for large-amplitude vibrations of plates and curved panels, part 2: identification and comparisons, *Int. J. Non-Linear Mech.* 85 (2016) 226–240, <http://dx.doi.org/10.1016/j.ijnonlinmec.2016.05.004>.
- [51] M. Amabili, Nonlinear damping in nonlinear vibrations of rectangular plates: Derivation from viscoelasticity and experimental validation, *J. Mech. Phys. Solids* 118 (2018) 275–292, <http://dx.doi.org/10.1016/j.jmps.2018.06.004>.
- [52] F. Aljiani, M. Amabili, P. Balasubramanian, S. Carra, G. Ferrari, R. Garziera, Damping for large-amplitude vibrations of plates and curved panels, part 1: Modeling and experiments, *Int. J. Non-Linear Mech.* 85 (2016) 23–40, <http://dx.doi.org/10.1016/j.ijnonlinmec.2016.05.003>.
- [53] A. Gupta, A. Ghosh, Isogeometric static and dynamic analysis of laminated and sandwich composite plates using nonpolynomial shear deformation theory, *Composites B* 176 (2019) 107295, <http://dx.doi.org/10.1016/j.compositesb.2019.107295>.
- [54] J.N. Reddy, Mechanics of Laminated Composite Plates and Shells: Theory and Analysis, CRC press, 2004, <http://dx.doi.org/10.1201/b12409>.
- [55] T. Caughey, M.E. O'Kelly, Classical normal modes in damped linear dynamic systems, *J. Appl. Mech.* 32 (3) (1965) 583–588, <http://dx.doi.org/10.1115/1.3643949>.
- [56] S. Krenk, Non-Linear Modeling and Analysis of Solids and Structures, Cambridge University Press, 2009, <http://dx.doi.org/10.1017/cbo9780511812163>.
- [57] M. Chandrashekhar, R. Ganguli, Nonlinear vibration analysis of composite laminated and sandwich plates with random material properties, *Int. J. Mech. Sci.* 52 (7) (2010) 874–891, <http://dx.doi.org/10.1016/j.ijmecsci.2010.03.002>.
- [58] M. Ganapathi, B. Patel, D. Makhecha, Nonlinear dynamic analysis of thick composite/sandwich laminates using an accurate higher-order theory, *Composites B* 35 (4) (2004) 345–355, [http://dx.doi.org/10.1016/s1359-8368\(02\)00075-6](http://dx.doi.org/10.1016/s1359-8368(02)00075-6).
- [59] L.V. Tran, J. Lee, H. Nguyen-Van, H. Nguyen-Xuan, M.A. Wahab, Geometrically nonlinear isogeometric analysis of laminated composite plates based on higher-order shear deformation theory, *Int. J. Non-Linear Mech.* 72 (2015) 42–52, <http://dx.doi.org/10.1016/j.ijnonlinmec.2015.02.007>.
- [60] J. Chen, D. Dawe, S. Wang, Nonlinear transient analysis of rectangular composite laminated plates, *Compos. Struct.* 49 (2) (2000) 129–139, [http://dx.doi.org/10.1016/s0263-8223\(99\)00108-7](http://dx.doi.org/10.1016/s0263-8223(99)00108-7).
- [61] J. Mantari, E. Bonilla, C.G. Soares, A new tangential-exponential higher order shear deformation theory for advanced composite plates, *Composites B* 60 (2014) 319–328, <http://dx.doi.org/10.1016/j.compositesb.2013.12.001>.
- [62] M. Touratier, An efficient standard plate theory, *Internat. J. Engrg. Sci.* 29 (8) (1991) 901–916, [http://dx.doi.org/10.1016/0020-7225\(91\)90165-y](http://dx.doi.org/10.1016/0020-7225(91)90165-y).
- [63] M. Ganapathi, T. Varadan, B. Sarma, Nonlinear flexural vibrations of laminated orthotropic plates, *Comput. Struct.* 39 (6) (1991) 685–688, [http://dx.doi.org/10.1016/0045-7949\(91\)90211-4](http://dx.doi.org/10.1016/0045-7949(91)90211-4).
- [64] B. Sarma, Nonlinear Free Vibrations of Beams, Plates and Nonlinear Panel Flutter (Ph.D. thesis, Ph.D. thesis), Department of Aerospace Engineering, IIT Madras, Chennai, 1987.
- [65] B. Adhikari, P. Dash, Geometrically nonlinear free vibration analysis of laminated composite plates: A finite element assessment of a higher order non-polynomial shear deformation theory, *Mech. Adv. Mater. Struct.* (2010) 1–12, <http://dx.doi.org/10.1080/15376494.2018.1553259>.
- [66] M. Amabili, C. Augenti, Nonlinear vibrations of rectangular plates with different boundary conditions: Theory and experiments, in: Applied Mechanics, ASMEDC, 2005, <http://dx.doi.org/10.1115/imece2005-82425>.

- [67] F. Alijani, F. Bakhtiari-Nejad, M. Amabili, Nonlinear vibrations of FGM rectangular plates in thermal environments, *Nonlinear Dynam.* 66 (3) (2011) 251–270, <http://dx.doi.org/10.1007/s11071-011-0049-8>.
- [68] T.Y. Tsui, P. Tong, Stability of transient solution of moderately thick plate by finite-difference method, *AIAA J.* 9 (10) (1971) 2062–2063, <http://dx.doi.org/10.2514/3.6463>.
- [69] T. Kant, J. Kommineni, Geometrically non-linear transient analysis of laminated composite and sandwich shells with a refined theory and c0 finite elements, *Comput. Struct.* 52 (6) (1994) 1243–1259, [http://dx.doi.org/10.1016/0263-8223\(94\)90267-4](http://dx.doi.org/10.1016/0263-8223(94)90267-4).
- [70] P. Ribeiro, Nonlinear vibrations of simply-supported plates by the p-version finite element method, *Finite Elem. Anal. Des.* 41 (9–10) (2005) 911–924, <http://dx.doi.org/10.1016/j.finel.2004.12.002>.
- [71] P.L. Ribeiro, Periodic vibration of plates with large displacements, *AIAA J.* 40 (1) (2002) 185–188, <http://dx.doi.org/10.2514/msdm98>.
- [72] C.K. Chiang, C. Mei, C.E. Gray, Finite element large-amplitude free and forced vibrations of rectangular thin composite plates, *J. Vib. Acoust.* 113 (3) (1991) 309–315, <http://dx.doi.org/10.1115/1.2930186>.